

1 Comparing open-source toolboxes for 2 processing and analysis of spike and local field 3 potentials data

4
5 **Valentina A. Unakafova^{1,*} and Alexander Gail^{1,2,3,4}**

6 ¹*Cognitive Neurosciences Laboratory, German Primate Center, Goettingen, Germany*

7 ²*Leibniz ScienceCampus, Primate Cognition, Goettingen, Germany*

8 ³*Georg-Elias-Mueller-Institute of Psychology, University of Goettingen, Goettingen, Germany*

9 ⁴*Bernstein Center for Computational Neuroscience, Goettingen, Germany*

10 *Correspondence: unakafovavalentina@gmail.com

11 **ABSTRACT.**

12 Analysis of spike and local field potential (LFP) data is an essential part of neuroscientific research. Today
13 there exist many open-source toolboxes for spike and LFP data analysis implementing various functionality.
14 Here we aim to provide a practical guidance for neuroscientists in the choice of an open-source toolbox best
15 satisfying their needs. We overview major open-source toolboxes for spike and LFP data analysis as well as
16 toolboxes with tools for connectivity analysis, dimensionality reduction and generalized linear modeling. We
17 focus on comparing toolboxes functionality, statistical and visualization tools, documentation and support
18 quality. To give a better insight, we compare and illustrate functionality of the toolboxes on open-access
19 dataset or simulated data and make corresponding MATLAB scripts publicly available.

20 **Keywords: spike data, LFP, toolbox, MATLAB, open-source, Python, dimensionality reduction, GLM**

21 **1 INTRODUCTION**

22 Analysis of spike and local field potential (LFP) data is an essential part of neuroscientific research (Brown
23 et al., 2004; Stevenson and Kording, 2011; Mahmud and Vassanelli, 2016). There are many already
24 implemented open-source tools and toolboxes for spike and LFP data analysis. However, ascertaining
25 whether functionality of the toolbox fits users' requirements is in many cases time-consuming. Often
26 neuroscientists are even not aware that some functionality is already implemented and start writing their own
27 scripts from scratch which takes time and is error-prone. We aim to provide a practical guidance for choosing
28 a proper toolbox on the basis of toolbox functionality, statistical and visualization tools, programming
29 language, availability of graphical user interface, support and documentation quality. Compared to the
30 existing reviews (Ince et al., 2009, 2010; Ince, 2012; Mahmud and Vassanelli, 2016; Timme and Lapish,
31 2018), we

- 32 - include in the comparison important toolboxes and tools not covered by earlier reviews (e.g., Brain-
33 storm, Elephant and FieldTrip);
- 34 - compare in detail common and discuss unique functionality of toolboxes;
- 35 - compare and illustrate functionality of the toolboxes on open-access datasets (Perich et al., 2018;
36 Lawlor et al., 2018; Lowet et al., 2015) and simulated data. For readers' convenience we make the
37 corresponding MATLAB scripts publicly available¹;
- 38 - overview specialized tools for dimensionality reduction and generalized linear modeling as they are
39 widely used in neuroscientific research (Cunningham and Byron, 2014; Truccolo et al., 2005);

¹<https://github.com/ValentinaUn/Testing-open-source-toolboxes>

- 40 - provide information about documentation and support quality for the toolboxes;
- 41 - indicate bibliometric information²: while popularity among users alone does not guarantee quality, it
- 42 can be an important indicator that toolbox's functions are easy-to-use and have been tested.

43 **Scope.** We include into our comparison major open-source³ toolboxes (see Table 1) for spike and LFP

44 data processing and analysis which have a valid link for downloading, documentation, scientific paper

45 describing toolbox's features or corresponding method, and which were updated during the last five years. In

46 Table 1 we provide a summary of the toolboxes we consider, we list all toolboxes with a brief description in

47 alphabetical order in Section 7 with paper reference and downloading link.

Table 1: Features of open-source toolboxes regarding graphical user interface (GUI), visualization tools, Import/Export of spike and LFP data in various file formats, e.g. recorded with different software/hardware, principal programming language, availability of documentation, number of citations, and support by updates at least once per year.

Toolbox, version	GUI	Visualization	Import/ Export	Language	Docu- mentation	Cited	Support
Brainstorm 3.4	+	+	+	MATLAB	+	>1000	+
Chronux 2.12 v03	-	+	+	MATLAB	+	>300	In part
Elephant v0.6.0	-	-	In part	Python	In part	<30	+
FieldTrip 23.11.18	-	+	+	MATLAB	+	>3000	+
gramm 2.25	-	+	-	MATLAB	+	<30	+
Spike Viewer 0.4.2	+	+	In part	Python	In part	<30	+
SPIKY 3.0	+	+	-	MATLAB Python	In part	<30	In part

48 Considered toolboxes were developed in MATLAB⁴ and Python⁵ languages which are popular in

49 neuroscientific community.

50 We have not listed in Table 1 toolboxes FIND (Meier et al., 2008), infotoolbox (Magri et al., 2009) and

51 STAtoolkit (Goldberg et al., 2009), since they are not available under the links provided by the authors

52 (accessed on 27.03.2019); toolboxes BSMART (Cui et al., 2008), DATA-Means (Bonomini et al., 2005),

53 MEA-tools (Egert et al., 2002), MEAbench (Wagenaar et al., 2005), sigTOOL (Lidierth, 2009), SPKTool

54 (Liu et al., 2011), STAR (Pouzat and Chaffiol, 2009), since they have not been updated during the last five

55 years (since 2008, 2005, 2007, 2011, 2011, 2011, and 2012, correspondingly); toolbox SigMate (Mahmud

56 et al., 2012) since it is in beta version; and toolbox OpenElectrophy (Garcia and Fourcaud-Trocmé, 2009)

57 which is not recommended for new users by the toolbox authors⁶.

58 **Documentation/Support.** We have indicated "In part" in Documentation column for Spike Viewer and

59 SPIKY since, compared to other toolboxes from Table 1, they do not provide a description of input parameters

60 for most of the functions. This complicates understanding of implementation details for programming-

61 oriented users that use only a part of the toolbox functionality in their analysis workflow. gramm toolbox

62 specifies function input parameters not in code comments but in separate documentation file⁷. Considered

63 version of Elephant provides only getting started tutorial, more tutorials are to be added⁸. Chronux and

64 SPIKY (MATLAB version) toolboxes are not uploaded to GitHub or other public version control systems,

²according to Google Scholar in March 2019 (<https://scholar.google.com>)

³when the code is available under a license which allows free redistribution and the creation of derived works

⁴<https://www.mathworks.com>

⁵<https://www.python.org>

⁶<https://github.com/OpenElectrophy/OpenElectrophy>

⁷<https://github.com/piermorel/gramm/blob/master/gramm%20cheat%20sheet.pdf>

⁸<https://elephant.readthedocs.io/en/latest/tutorial.html>

65 which prevents from tracking version differences and smoothly reporting bugs (Python version of SPIKY is
66 on GitHub⁹).

67 **Import/Export.** We have indicated “In part” in Import/Export column for Elephant and Spike Viewer
68 toolboxes since they require Neo-based Python package^{10,11} (Garcia et al., 2014) for the support of spike file
69 formats (Spike2, NeuroExplorer, AlphaOmega, Blackrock, Plexon etc.). This Neo-based package is popular
70 in neuroscientific society but requires either a separate installation or data conversion to Neo-compatible data
71 format. Brainstorm, Chronux and FieldTrip support working with several spikes file formats (e.g. Blackrock,
72 CED, Neuralynx, Plexon etc.)¹² as well as working with data from MATLAB workspace or stored as .mat
73 files. SPIKY and gramm support working with data from MATLAB workspace; SPIKY also supports
74 working with data stored in .mat and .txt file formats.

75 **Compatibility.** Chronux under Macintosh operating system requires recompilation of the locfit¹³ and
76 spikesort packages. All other listed toolboxes are supported by Microsoft Windows, Macintosh and Linux
77 operating system. Chronux, FieldTrip, gramm and SPIKY require MATLAB installation, Elephant requires
78 Python installation, Brainstorm and Spike Viewer require neither MATLAB nor Python installation.

79 **Test dataset.** We consider for illustration of toolboxes functionality an open-access dataset (Lawlor et al.,
80 2018; Perich et al., 2018) and refer to this dataset further as “test dataset”. The dataset contains extracellular
81 recordings from premotor (PMd) and primary motor (M1) cortex from a macaque monkey in a sequential
82 reaching task where monkey controlled a computer cursor using arm movements. A visual cue specified the
83 target location for each reach. The monkey receives a reward after making four correct reaches to the targets
84 within the trial.

85 In Sections 2 and 3, we compare toolboxes for the general spike and LFP data analysis, correspondingly.
86 In Section 4, we compare tools for the analysis of synchronization and connectivity in spike and LFP data.
87 Each of Sections 2-4 is subdivided into two subsections: first, we compare common toolboxes functionality,
88 then we discuss unique toolboxes functionality, i.e. functionality implemented only in one of the toolboxes
89 under comparison. In Section 5, we compare toolboxes with specialized tools for dimensionality reduction
90 and generalized linear modeling. Finally, we summarize the comparisons in Section 6. In Section 7, we list
91 all the considered toolboxes in alphabetical order with links for toolbox downloading and brief descriptions.
92 We do not consider in this review toolboxes specializing on spike sorting and modeling spiking activity. For
93 this we refer to (Ince et al., 2010; Mahmud and Vassanelli, 2016) and web-reviews^{14,15,16} correspondingly.

94 2 TOOLBOXES FOR SPIKE DATA PROCESSING AND ANALYSIS

95 In Table 2 we compare major open-source toolboxes for spike data analysis, both for point-process data
96 and for spike waveforms. Functionality related to synchronization and connectivity analysis (e.g. cross-
97 correlation, coherence, joint peri-stimulus time histogram, spike-LFP phase-coupling and dissimilarity
98 measures etc.) will be covered in Section 4, and functionality related to dimensionality reduction and
99 generalized linear modeling in Section 5.

100 From Table 1 and 2 one can see that Brainstorm, Chronux and FieldTrip toolboxes provide more versatile
101 functionality (see also below) than others, are highly cited, well-documented and allow import from many
102 file formats. The Elephant toolbox has versatile functionality (see Subsection 2.2) but it does not have built-in
103 visualization tools (Elephant provides visualization examples in the documentation using matplotlib
104 Python library). Compared to other toolboxes from Table 2,

⁹<https://github.com>

¹⁰<https://github.com/NeuralEnsemble/python-neo>

¹¹<http://neuralensemble.org/neo/>

¹²see <https://neuroimage.usc.edu/brainstorm/Introduction>, Chronux folder dataio and <http://www.fieldtriptoolbox.org/dataformat> for details, correspondingly

¹³One can recompile locfit by running `locfit/source/compile.m`

¹⁴<https://simonster.github.io/SpikeSortingSoftware/>

¹⁵<https://www.cnsorg.org/software>

¹⁶https://grey.colorado.edu/emergent/index.php/Comparison_of_Neural_Network_Simulators

Table 2: Comparing open-source spike data processing and analysis toolboxes. CV2 – measure of inter-spike variability (Holt et al., 1996), ISIH – Inter-Spike Interval Histogram, locfit – local regression and likelihood based analyses (Bokil et al., 2010; Loader, 2006), LV – measure of Local Variation (Shinomoto et al., 2003), MTF – MultiTaper Fourier transform for point-process data (Jarvis and Mitra, 2001; Bokil et al., 2010), PSTH – Peri-Stimulus Time Histogram

Toolbox	ISIH	PSTH	Raster plots	Spike sorting	Tuning curves	Statistical tools	Unique features
Brainstorm	–	–	+	+	+	+	–
Chronux	+	+	–	–	–	+	locfit, MTF
Elephant	+	+	–	–	–	+	CV2, Fano factor, LV
FieldTrip	+	+	+	+	–	+	waveform statistics
gramm	–	+	+	–	+	+	–
Spike Viewer	+	+	+	–	–	–	–
SPIKY	–	+	+	–	–	–	–

- 105 - Brainstorm and FieldTrip include detailed documentation with tutorials and examples (documentation
106 of other toolboxes from Table 2 has less examples/tutorials for spike data analysis) and have either a
107 forum¹⁷ or a discussion list¹⁸ where users can ask questions on data analysis; both toolboxes regularly
108 hold hands-on courses^{19,20}, while other toolboxes from Table 2 provide neither forums nor courses;
- 109 - Brainstorm and FieldTrip are actively developing by including new functionality;
- 110 - FieldTrip provides many descriptive and inferential statistics mostly not requiring MATLAB statistical
111 toolbox (Brainstorm provides statistical tools²¹ without examples for spike data analysis²² and these
112 statistical functions are not part of spike data analysis functions, different to how it is often done in
113 FieldTrip and Chronux; Spike Viewer and SPIKY do not provide statistical tools for general spike data
114 analysis);
- 115 - FieldTrip and gramm allow versatile data plots customization (color maps, line widths, smoothing,
116 errorbars etc.); while gramm provides better and quicker general visualization tools, FieldTrip provides
117 plotting customization specific for spike data analysis (conditions/interval/trials/channels and optimal
118 bin size selection);
- 119 - for programming-oriented users, Chronux and FieldTrip provide, to our opinion, most convenient and
120 well-commented data analysis pipeline with clear uniform data structure (other toolboxes from Table 2
121 are lacking at least one of three following components: detailed code comments with description of
122 input/output parameters, uniform data structure throughout the analysis pipeline, modular function
123 design allowing to easily adapt them into analysis workflow). Chronux reference documentation in the
124 function description provides a list of functions which are called from the function and from which the
125 function is called, this is convenient for programming-oriented users.

¹⁷<https://neuroimage.usc.edu/forums/>

¹⁸http://www.fieldtriptoolbox.org/discussion_list/

¹⁹<http://www.fieldtriptoolbox.org/workshop/>

²⁰<https://neuroimage.usc.edu/brainstorm/Training>

²¹<https://neuroimage.usc.edu/brainstorm/Tutorials/Statistics>

²²<https://neuroimage.usc.edu/brainstorm/Tutorials/Statistics>

126 2.1 Comparing common tools: peri-stimulus time-histogram, raster plot, inter- 127 spike interval histogram and spike sorting

128 In this subsection we compare most common spike data analysis functions: peri-stimulus time histogram
 129 (PSTH), raster plot, inter-spike interval histogram (ISIH) and spike sorting algorithms for toolboxes from
 130 Table 2. Regarding visualization, the gramm visualization toolbox stands out with its publication-quality
 131 graphics, which helps avoiding major post-processing. This is illustrated in Figure 1, where we compare
 132 PSTH and raster plots for test dataset produced in FieldTrip and gramm toolboxes, both of which provide
 133 most adjustable plot properties compared to other toolboxes from Table 2 (see below a detailed comparison).

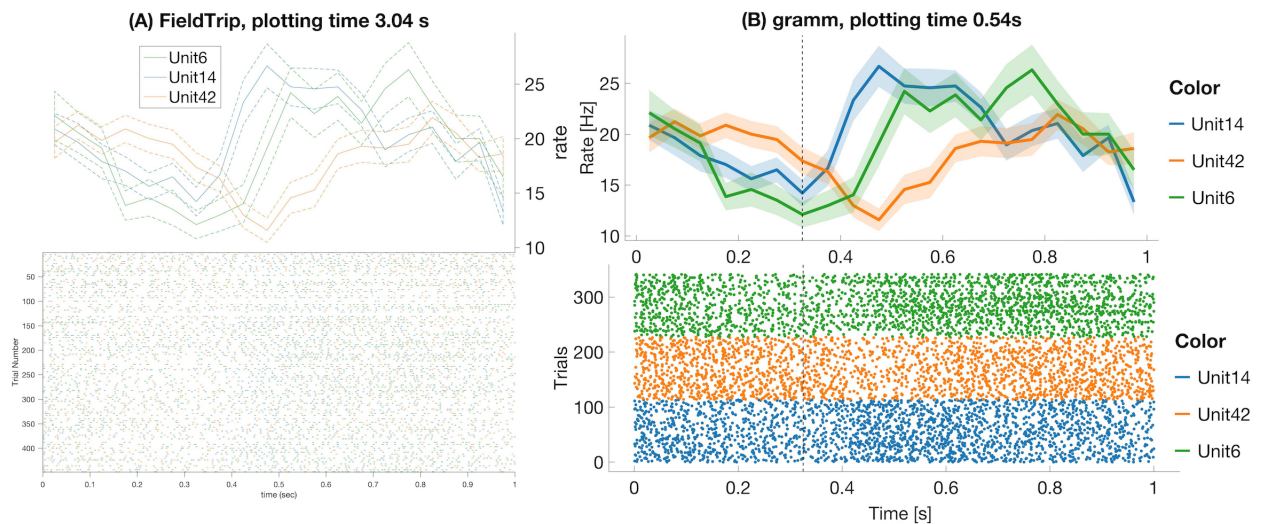


Figure 1: FieldTrip (A) and gramm (B) provide most adjustable peri-stimulus (PSTH) and raster plots properties (plotting time is averaged over 1000 runs, MATLAB 2016a, here and later for processor 3.2 GHz Intel Core i5 with 16GB RAM) among toolboxes from Table 2. We considered 50 ms bin size, M1 units 6, 14, 42, monkey MM for the test dataset. PSTHs are presented with standard error of the mean, neural activity is aligned to trial start for reaches toward the second target in the trial. FieldTrip build-in tools do not allow to adjust font size in a raster plot and line width in a PSTH plot (one has to do it manually with MATLAB tools), and do not allow to plot raster and PSTH in separate figures (though one can plot spike densities in a separate figure). Advantages of gramm toolbox for PSTH and raster plots are quick plotting, raster plots separation for different units, vertical dashed lines for showing event times of the experiment protocol, and smooth adjustment of line width, font size, color maps, errorbar, components positions, etc.

134 We do not provide raster plots and PSTH plots for other toolboxes from Table 2 with visualization tools
 135 since

- 136 - Brainstorm does not provide PSTH plots; raster plots are available only for one unit per figure²³;
- 137 - Chronux does not provide raster plots and allows to plot only smoothed PSTH for one unit per figure
 138 without built-in tools to adjust line width, font size, colors etc.;
- 139 - in SPIKY raster and PSTH plots are available only for one unit per figure without built-in tools to
 140 adjust line width, marker size, font style and size, colors (Kreuz et al., 2015, Figure 2) and without
 141 confidence intervals for PSTHs;
- 142 - in Spike Viewer PSTH plots are available without confidence intervals²⁴.

143 Regarding statistical tools when computing PSTHs, Chronux computes PSTH for adaptive or user-defined
 144 kernel width with Poisson error or bootstrapped over trials (both with doubled standard deviation error).

²³<https://neuroimage.usc.edu/brainstorm/e-phys/functions>

²⁴<https://spyke-viewer.readthedocs.io/en/latest/>

145 Elephant computes PSTH for fixed user-defined bin size without additional statistics (note that Elephant
146 provides many kernel functions for convolutions such as rectangular, triangular, Guassian, Laplacian,
147 exponential, alpha function etc.). FieldTrip computes PSTH for optimal (by Scott's formula (Scott, 1979)) or
148 user-defined bin width with variance computed across trials. Besides, FieldTrip, different to other toolboxes
149 from Table 2, allows statistical testing on PSTHs for different conditions or subjects²⁵ with a parametric
150 statistical or a non-parametric permutation test. Brainstorm provides this functionality by calling FieldTrip
151 functions. gramm allows to compute PSTHs with (bootstrapped) confidence intervals, standard error of the
152 mean, standard deviation etc²⁶ only for user-defined bin width. Spike Viewer and SPIKY compute PSTH
153 only for user-defined bin width and do not compute statistics for PSTHs across trials.

154 In Figure 2 we compare visualization of ISIH provided by FieldTrip and Spike Viewer since other
155 toolboxes from Table 2 do not provide ISIH visualization (Brainstorm, Chronux and Elephant compute ISIH
156 without visualization, see details below).

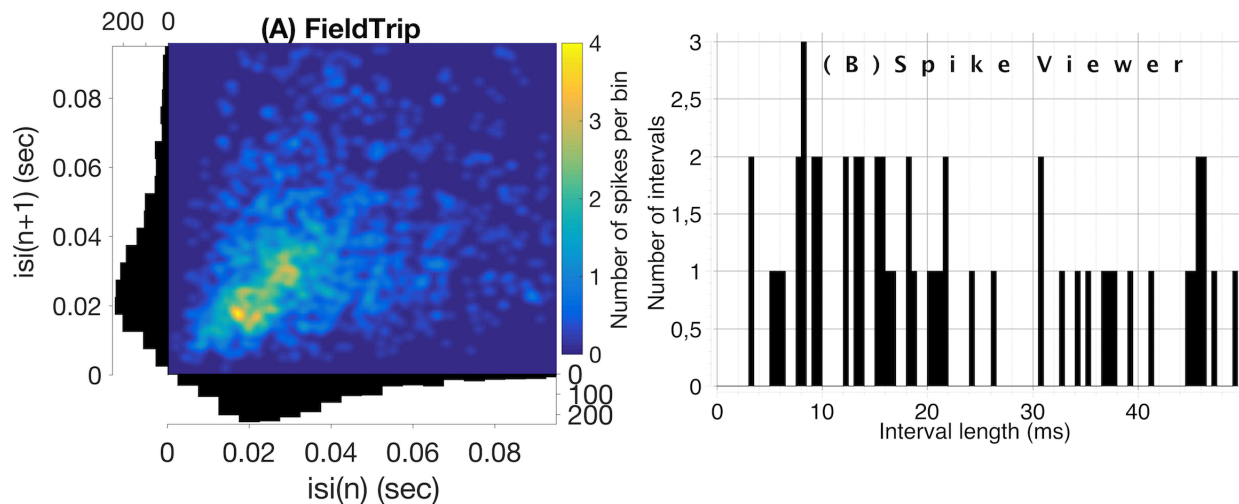


Figure 2: Compared to Spike Viewer (B), FieldTrip (A) provides also a second-order statistic on inter-spike interval histogram (ISIH). We considered test dataset (M1 unit 14 aligned to trial start for reaches towards the first target, monkey MM) for FieldTrip plot and Spike Viewer test dataset for Spike Viewer plot. Font sizes in FieldTrip have been adjusted with MATLAB tools since FieldTrip built-in tools do not provide this option.

157 Regarding statistical tools when computing ISIH, FieldTrip computes ISIH with a coefficient of variation
158 (a ratio of the standard deviation to the mean), Shinomoto's local variation measure (Shinomoto et al., 2005)
159 or a shape scale for a gamma distribution fit. Chronux computes ISIH with two standard deviations away
160 from the mean calculated using jackknife resampling. Elephant computes ISIH with a coefficient of variation.
161 Spike Viewer does not compute statistics on ISIH.

162 Brainstorm and FieldTrip provide spike sorting algorithms including spike detection and extraction, i.e.,
163 using time-continuous broadband data as input. Spike sorting package is no longer provided by Chronux.
164 Brainstorm implements supervised and unsupervised spike sorting according to the methods WaveClus
165 (Quiroga et al., 2004), UltramegaSort2000 (Hill et al., 2011; Fee et al., 1996), KiloSort (Pachitariu et al.,
166 2016) and Klusters (Hazan et al., 2006). FieldTrip implements k-means and Ward (for several Ward distances)
167 sorting methods. While Chronux and FieldTrip do not provide tutorials on spike sorting, Brainstorm has a
168 detailed tutorial²⁷.

169 Brainstorm provides computing and visualization of tuning curves: they are plotted with one figure per
170 unit for selected units, conditions and time interval but without customization of font size, line width and
171 colors, no variance statistic across trials is computed²⁸. gramm toolbox provides visualization of tuning

²⁵http://www.fieldtriptoolbox.org/reference/ft_timelockstatistics/

²⁶<https://github.com/piermorel/gramm/blob/master/gramm>

²⁷<https://neuroimage.usc.edu/brainstorm/e-phys/SpikeSorting?highlight=%28sorting%29>

²⁸<https://neuroimage.usc.edu/brainstorm/e-phys/functions>

172 curves including fits from MATLAB curve smoothing toolbox and user-defined functions (also in polar
 173 coordinates) with (bootstrapped) confidence intervals, standard error of the mean, standard deviation etc. As
 174 the considered gramm version is not focused on spike data analysis, firing rates averaged per condition need
 175 to be computed prior to tuning curves visualization (see example in our open MATLAB script).

176 2.2 Description of unique tools

177 In this subsection we discuss unique tools of toolboxes from Table 2, e.g. fitting tools, and higher order
 178 statistics (variability and spectral measures) on spike timing.

179 Chronux provides two unique tools: local regression package (locfit) and point-process spectrograms.
 180 locfit is based on local regression methods (Loader, 2006; Parikh, 2009; Hayden et al., 2009) and provides a
 181 set of methods for fitting functions and probability distributions to noisy data. The idea of local regression is
 182 that the estimated function is approximated by a low order polynomial in a local neighborhood of any point
 183 with polynomial coefficients estimated by the least mean squares method (Bokil et al., 2010). In (Bokil et al.,
 184 2010; Loader, 2006) local regression methods are motivated by their simplicity, non-parametric approach to
 185 kernel smoothing and by reducing the bias at the boundaries which is present in kernel smoothing methods.
 186 On the other hand, it was shown that fixed and variable kernel methods (Shimazaki and Shinomoto, 2010,
 187 Algorithm 2, Appendix A.2) as well as Abramson’s adaptive kernel method (Abramson, 1982) outperform
 188 locfit for simulated data examples (Shimazaki and Shinomoto, 2010).

189 Point-process spectrograms are usually used to illustrate rhythmic properties of otherwise stochastic
 190 spiking patterns rather than for statistical inference (Deng et al., 2013). We refer to (Hurtado et al., 2004,
 191 2005) regarding methods to evaluate statistical significance of point-process spectral estimators and to (Jarvis
 192 and Mitra, 2001; Rivlin-Etzion et al., 2006) for a critical discussion. Chronux provides the only open-source,
 193 to our knowledge, implementation of point-process spectral estimates which is implemented according to
 194 (Jarvis and Mitra, 2001; Rivlin-Etzion et al., 2006, Section 4, Formula 11), see example of usage in our open
 195 MATLAB script.

196 Elephant provides several statistical measures for spike timing variability such as Fano factor, CV2
 197 measure of inter-spike variability (Holt et al., 1996) and a measure of local variation (Shinomoto et al., 2003)
 198 which were introduced as substitutes of classical coefficient of variation to overcome its sensitivity to firing
 199 rate fluctuations between trials (Shinomoto et al., 2005).

200 FieldTrip allows to compute mean average spike waveform and its variance across trials, one can
 201 optionally align waveforms based on their peaks, rejects outlier waveforms and interpolate the waveforms.

202 3 TOOLBOXES FOR LFP DATA ANALYSIS

203 In Table 3 we compare open-source toolboxes for processing and analysis of local field potential (LFP) data.
 204 Functionality related to synchronization and connectivity analysis will be discussed in Section 4.

Table 3: Comparing open-source toolboxes for processing and analysis of LFP data. FFT – Fast Fourier Transform

Toolbox	Digital filtering	De-trending	FFT	Hilbert transform	Line noise removal	Multitaper methods	Wavelet transform	Statistical tools
Brainstorm	+	+	+	+	+	+	+	+
Chronux	–	+	+	–	+	+	–	+
Elephant	+	–	+	+	–	–	+	–
FieldTrip	+	+	+	+	+	+	+	+

205 From Table 3 one can see that Brainstorm and FieldTrip toolboxes provide most versatile functionality
 206 for LFP data analysis. Compared to other toolboxes from Table 3,

- 207 - FieldTrip provides most flexible and versatile digital filtering (in particular, a fast and accurate line
208 noise removal technique) and spectral analysis tools (see details in Subsection 3.1);
- 209 - Brainstorm^{29,30} and FieldTrip^{31,32} provide detailed tutorials with guidance on parameter choice and
210 examples for digital filtering and spectral analysis. Chronux provides examples on parameter choice
211 for spectral analysis in manuals³³ (Pesaran, 2008);
- 212 - Brainstorm and Elephant provide fast implementation of Morlet wavelet transform (see details in
213 Subsection 3.1);
- 214 - Brainstorm, Chronux and FieldTrip provide statistical tools for computing variance across trials and
215 for comparing between conditions when estimating spectra; Elephant does not compute statistics on
216 the estimated spectra;
- 217 - Brainstorm and FieldTrip allow adjustment of plot properties for spectral analysis such as baseline
218 correction, trials and channels selection, colormaps and interactive selection of spectrogram part for
219 further processing. Neither Chronux nor Elephant provide these options. Compared to Brainstorm,
220 FieldTrip also allows to adjust font sizes, titles, plot limits etc.

221 3.1 Comparing common tools: filtering, detrending and spectral analysis

222 Digital filtering is implemented in Brainstorm, FieldTrip and Elephant toolboxes. Compared to toolboxes
223 from Table 3, MATLAB and Python themselves provide more flexible filtering tools. Yet, it is convenient to
224 have filtering within the toolbox pipeline. First, it allows to avoid extra conversion from toolbox's format
225 to MATLAB/Python and back. Second, toolboxes allow simplified setting of filter parameters for typical
226 neuroscientific datasets and offer tutorials for their choice for non-experienced users.

227 Brainstorm, FieldTrip and Elephant toolboxes provide low/high/band-pass and band-stop filters for
228 user-defined frequencies.

- 229 - Brainstorm provides Finite Impulse Response (FIR) filters with Kaiser window based on `kaiserord`
230 functions from MATLAB Signal Processing Toolbox (Octave-based alternatives are used if this toolbox
231 is not available). The user can set 40 or 60 dB stopband attenuation, data are padded with zeros at edges
232 with a half of filter order length (according to the description of the filtering `bst_bandpass_hfilter`
233 function used by default);
- 234 - Elephant provides Infinite Impulse Response (IIR) Butterworth filtering with adjustable order using
235 `scipy.signal.filtfilt` (with default padding parameters) or `scipy.signal.lfilter` standard
236 Python functions;
- 237 - FieldTrip provides the most flexible filtering tools with user-defined filter type (Butterworth IIR,
238 window sinc FIR filter, FIR filter using either standard MATLAB `fir1` or `firls` function from Signal
239 Processing Toolbox or frequency-domain filter using standard `fft` and `ifft` MATLAB functions),
240 padding type and optional parameters such as window type (Hanning, Hamming, Blackman, Kaiser),
241 filter order and direction, transition width, passband deviation, stopband attenuation etc.³⁴. An
242 automatic tool to deal with filter instabilities (which MATLAB 2016a, to our knowledge, does not
243 provide) is implemented by either recursively reducing filter order or recursively splitting the filter into
244 sequential filters.

²⁹<https://neuroimage.usc.edu/brainstorm/Tutorials/ArtifactsFilter>

³⁰<https://neuroimage.usc.edu/brainstorm/Tutorials/TimeFrequency>

³¹http://www.fieldtriptoolbox.org/example/determine_the_filter_characteristics/

³²<http://www.fieldtriptoolbox.org/tutorial/timefrequencyanalysis/>

³³<http://chronux.org>

³⁴http://www.fieldtriptoolbox.org/reference/ft_preprocessing

245 Brainstorm, Chronux and FieldTrip also provide specific tools for line noise removal. Brainstorm reduces
 246 line noise with IIR notch filter (employing either `filtfilt` function from MATLAB Signal Processing
 247 toolbox or MATLAB `filter` function). Chronux reduces line noise using Thomson's regression method
 248 for detecting sinusoids (Thomson, 1982). FieldTrip reduces line noise by two alternative methods: with
 249 a discrete Fourier transform (DFT) filter (by fitting a sine and cosine at user-defined line noise frequency
 250 and subsequently subtracting estimated components) or by spectrum interpolation (Mewett et al., 2004). In
 251 Figure 3 we compare 60 Hz line noise removal by Chronux, FieldTrip and Brainstorm toolboxes on the basis
 252 of an example provided by MATLAB³⁵ for open-loop voltage across the input of an analog instrument in
 253 the presence of 60 Hz power-line noise. One can see that FieldTrip selectively and successfully attenuates
 254 60 Hz while Brainstorm does not fully suppress 60 Hz, Chronux suppresses also frequencies around 62
 255 Hz, the MATLAB solution contains some remaining oscillations in the beginning of the signal, which is
 256 also reflected in the periodogram by a slight inaccuracy around 61-62 Hz. In Figure 3 (C) we present mean
 257 squared error (MSE) between power spectrum values of the original and estimated signal except the values
 258 estimated in 0.2 Hz vicinity of 60 Hz.

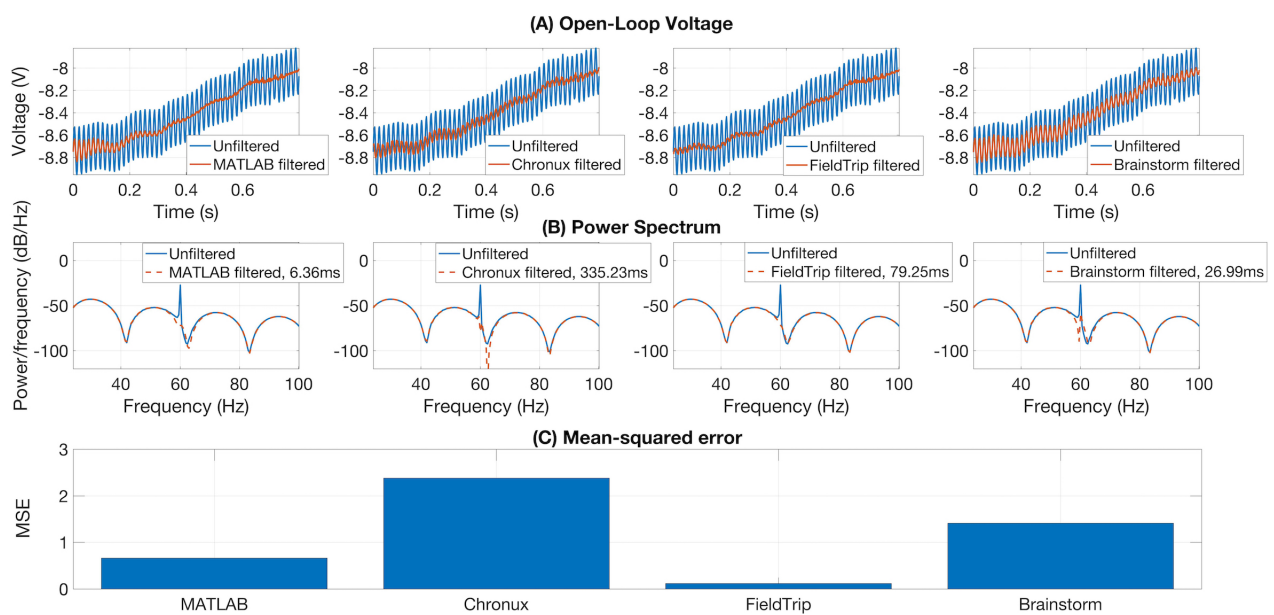


Figure 3: FieldTrip (discrete Fourier transform filter, default parameters) provides the fastest and the most accurate line noise removal compared to MATLAB solution (Butterworth notch filter with 2 Hz width), Chronux (default 5 tapers, bandwidth 3) and Brainstorm (IIR notch filter with 1 Hz width). Filtering times are averaged over 1000 runs, MATLAB 2016a.

259 Brainstorm, Chronux and FieldTrip provide detrending tools. Brainstorm removes a linear trend from the
 260 data, Chronux detrending employs local linear regression³⁶, whereas FieldTrip detrending uses a general
 261 linear model approach and removes mean and linear trend from the data (by fitting and removing an N th
 262 order polynomial from the data)³⁷: Brainstorm, Chronux and FieldTrip offer similar performance in terms
 263 of processing time and trend removal accuracy for a simple MATLAB example³⁸ (see our open MATLAB
 264 code).

265 Compared to the classic Fourier transform, multitaper methods provide more convenient control of time
 266 and frequency smoothing (Percival and Walden, 1993; Mitra, 2007). Spectral decomposition with Morlet
 267 wavelets provides a convenient way of achieving a time-frequency resolution trade-off (van Vugt et al., 2007),
 268 since it is inherent to the method that wavelets are scaled in time to vary resolution in time and frequency,

³⁵<https://www.mathworks.com/help/signal/ug/remove-the-60-hz-hum-from-a-signal.html>

³⁶http://chronux.org/chronuxFiles/Documentation/chronux/spectral_analysis/continuous/locdetrend.html

³⁷http://www.fieldtriptoolbox.org/reference/ft_preproc_detrend/

³⁸https://de.mathworks.com/help/matlab/data_analysis/detrending-data.html

269 see (van Vugt et al., 2007) for a comparison of multitaper and wavelet methods and (Bruns, 2004) for a
270 comparison of wavelet, Hilbert and Fourier transform. Equivalent time-frequency trade-offs can also be
271 implemented with short-time Fourier or Hilbert methods via variable-width tapers (Bruns, 2004).

272 Chronux and FieldTrip provide multitaper power spectrum estimation using Thomson's method (Thomson, 1982; Percival and Walden, 1993; Mitra and Pesaran, 1999) with Slepian sequences (Slepian and Pollak, 1961). Additionally to this, FieldTrip allows also more conventional tapers (e.g. Hamming, Hanning). In
273 FieldTrip, the user defines frequencies and time interval of interest, width of sliding window and of frequency
274 smoothing. In Chronux, the user defines bandwidth product and number of tapers to be used (see (Prieto
275 et al., 2007) for a discussion of multitapers parameter choice).

276 Brainstorm, Elephant and FieldTrip implement complex-valued Morlet transform. FieldTrip provides
277 time-frequency transformation using Morlet waveforms either with convolution in the time domain or with
278 the multiplication in the frequency domain. Brainstorm and Elephant implement convolution in the time
279 domain. FieldTrip implements Morlet wavelet transformation methods based on (Tallon-Baudry et al., 1997),
280 the user defines the wavelet width in number of cycles and optionally wavelet length in standard deviations
281 of the implicit Gaussian kernel. In Brainstorm the user sets the central frequency and temporal resolution.
282 Elephant implements Morlet wavelets according to (Le Van Quyen et al., 2001; Farge, 1992), where the user
283 sets central Morlet frequencies, size of the mother wavelet and padding type.

284 Different to other toolboxes from Table 3 FieldTrip also implements Fourier transform on the coefficients
285 of the multivariate autoregressive model estimated with FieldTrip tools (see Subsection 4.1 for more details
286 on MVAR implementation in FieldTrip).

287 Elephant does not compute statistics on estimated power spectrum whereas Chronux and FieldTrip
288 compute confidence intervals and standard error, correspondingly, in a standard way or with jackknife
289 resampling. To compare spectrum estimates for different conditions or subjects, Chronux provides a
290 two-group test and FieldTrip performs a parametric statistical test, a non-parametric permutation test or a
291 cluster-based permutation test (Brainstorm includes these FieldTrip statistical functions).

292 MATLAB R2016a, compared to Chronux, FieldTrip and Brainstorm,

- 293 - does not provide detailed tutorials for multitaper and wavelet parameters choice;
- 294 - does not have built-in tools for computing average spectrogram across trials;
- 295 - does not have built-in tools for generating multitaper spectrograms;
- 296 - uses exclusively short-time Fourier transform for standard spectrogram plotting.

297 In Figure 4 we compare spectrum estimation methods implemented in Brainstorm (A), Chronux (B),
298 Elephant (C), FieldTrip (D-F) and MATLAB (G-H) for two simulated signals, $x_1(t)$ and $x_2(t)$.

299 We generate $x_1(t)$ as a sum of sines and $x_2(t)$ by sinusoidal frequency modulation, see Eq. 1-2. We add
300 normally distributed pseudo-random values with zero mean to the second half of both signals:

$$301 \quad x_1(t) = \sin(2\pi 8t) + \sin(2\pi 20t) + \sin(2\pi 40t) + \sin(2\pi 60t) + \varepsilon(t) \quad (1)$$

$$302 \quad x_2(t) = \cos(2\pi 40t + 6 \sin(2\pi 2t)) + \varepsilon(t) \quad (2)$$

$$\varepsilon(t) = \begin{cases} 0, & \text{for } t = 1, 2, \dots, 2000, \\ \sim N(0, 1), & \text{for } t = 2001, 2002, \dots, 4000. \end{cases} \quad (3)$$

The instantaneous frequency of the signal $x_2(t)$ is defined by the following equation (Granlund, 1949):

$$f(t) = 40 + 12 \cos(2\pi 2t). \quad (4)$$

303 To compare quantitatively the spectra estimated by the toolboxes we compute power spectrum values of
304 the ideal signal by setting maximum spectrum values at theoretical frequencies of the signals x_1 (8, 20, 40

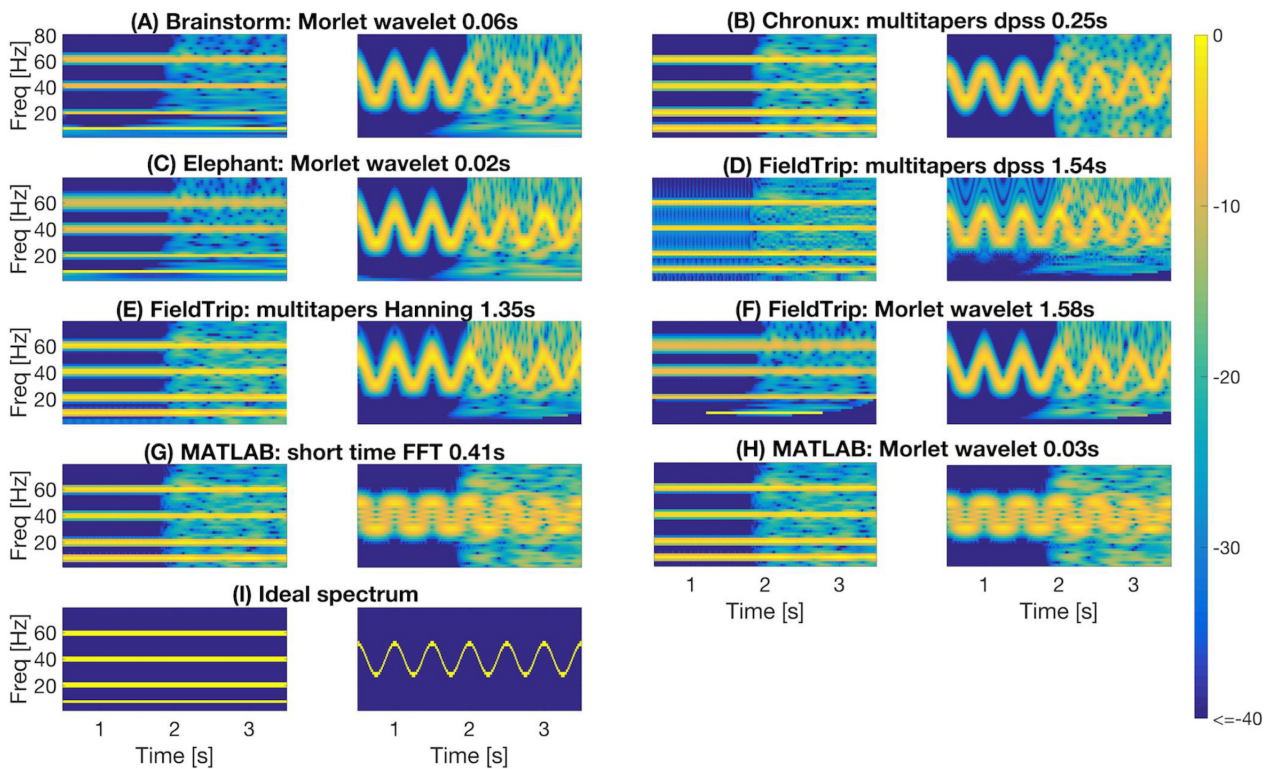


Figure 4: Comparing spectral analysis tools provided by the toolboxes. For each toolbox we plot estimated spectrum of signal x_1 (left subpanel) and of signal x_2 (right subpanel). For short-time FFT we used 0.512 s moving window with 0.001s step. For multitaper methods we used in Chronux a single taper with time bandwidth product 2 (left) and 8 (right); in FieldTrip a single taper with 2 Hz (left) and $0.1F$ (right) frequency smoothing for time window 0.512s (left) and $8/F$ (right) at frequency F . For wavelet methods we used in MATLAB and Brainstorm central frequency 4 (left) and 1.5 (right) Hz; in Elephant and FieldTrip 20 (left) and 10 (right) cycles wavelets resulting in the spectral bandwidth $F/10$ (left) and $F/5$ (right) Hz at frequency F . Spectrum estimating times were averaged over 1000 runs in MATLAB 2016a.

305 and 60 Hz) and x_2 (given by Eq. 4) and minimum at all other frequencies. When setting ideal power spectrum
 306 values we allow bandwidth of 1 Hz, i.e. we set the maximum power spectrum values also at neighboring
 307 frequencies. Then we compare in Figure 5 the estimated spectrum values with the ideal spectrum values
 308 using mean squared error and two-dimensional Pearson correlation coefficient as suggested in (Rankine
 309 et al., 2005).

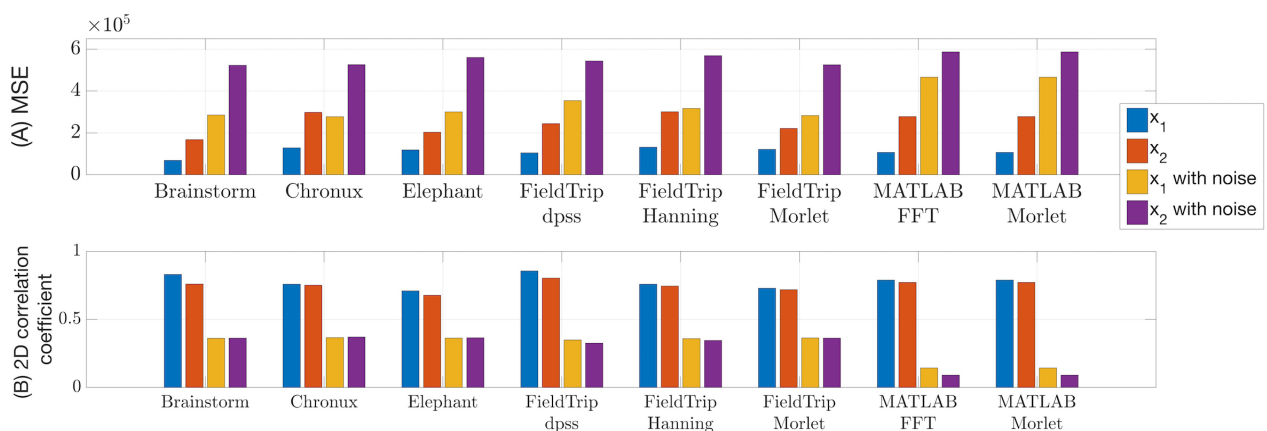


Figure 5: Mean squared error (A) and two-dimensional Pearson correlation coefficient (B) values between estimated and ideal spectra. These measures were computed for the time span from 1 to 3 s for the signals generated according to Eqs. 1-2. The lower MSE and the higher correlation coefficient are, the closer is the estimated spectrum to the ideal spectrum.

310 From Figures 4-5 we conclude that

311 - MATLAB standard spectrogram tools are less robust with respect to noise than spectrum estimation
312 provided by the toolboxes from Table 3 for the signal x_2 with changing frequencies;

313 - while Brainstorm, Chronux, Elephant and FieldTrip provide equally good accuracy of spectra estima-
314 tion, Brainstorm and Elephant provide the fastest computing tools (see spectra computing times in
315 subplot titles of Figure 4).

316 See in our open MATLAB script an example of spectral analysis with averaging over trials for real-world
317 LFP data (Lowet et al., 2015).

318 3.2 Description of unique tools

319 Compared to other toolboxes from Table 3, Chronux provides several unique features for specialized
320 computations (Bokil et al., 2010) such as space-frequency singular value decomposition (SVD) for univariate
321 and multivariate continuous signals: for theoretical details we refer to (Mitra and Pesaran, 1999) and for an
322 example of possible application to (Makino et al., 2017; Prechtl et al., 1997). Space-frequency SVD can be
323 applied to the space-time data as, for example, in (Prechtl et al., 1997), where space-frequency SVD has
324 been applied for spectral analysis of transmembrane potentials optically recorded in pixels distributed in
325 space. Chronux also provides computation of multitaper spectral derivatives and stationarity statistical test
326 for continuous processes based on quadratic inverse theory.

327 Elephant provides computing of the current source density from LFP data using electrodes with 2D or
328 3D geometries.

329 4 TOOLBOXES WITH SYNCHRONIZATION AND CONNECTIVITY ANALYSIS TOOLS

330 In Table 4 we compare open-source toolboxes providing tools for spike-spike, field-field (LFP-LFP) or
331 spike-field (spike-LFP) synchronization and connectivity analysis. We refer to (Blinowska, 2011; Bastos and
332 Schoffelen, 2016) for reviews of functional connectivity analysis methods and their interpretational pitfalls
333 (e.g. common reference, common input, volume conduction or sample size problems). We do not include in
334 Table 4 the connectivity toolboxes ibTB (Magri et al., 2009) and Toolconnect (Pastore et al., 2016), since
335 they are not available under the links provided by the authors (accessed on 27.03.2019). We also do not
336 list in Table 4 the following connectivity analysis toolboxes that are not focused on spike and LFP data
337 analysis: Inform (Moore et al., 2017), HERMES (Niso et al., 2013), JIDT (Lizier, 2014), MVGC (Barnett
338 and Seth, 2014), MuTe (Montalto et al., 2014), PyEntropy (Ince et al., 2009), SIFT (Delorme et al., 2011)
339 and TrenTool (Lindner et al., 2011). TrenTool toolbox has a FieldTrip-compatible data structure.

340 Compared to other toolboxes from Table 4,

341 - Brainstorm, Elephant and FieldTrip provide most versatile set of connectivity measures: while Field-
342 Trip provides many classic and recent pairwise connectivity and synchronization measures, Elephant
343 provides tools for multivariate analysis of high-order correlations in spike trains (see Subsections 4.1-
344 4.2);

345 - Brainstorm tutorials for connectivity measures are actively developing³⁹; Chronux has examples
346 for connectivity measures for real-world data in tutorial presentations; FieldTrip provides detailed
347 tutorials on connectivity analysis for simulated and real-world data; Elephant provides examples for
348 connectivity measures with simulated data;

³⁹<https://neuroimage.usc.edu/brainstorm/Tutorials/Connectivity>

Table 4: Comparison of connectivity analysis toolboxes for spike and LFP data. DTF – Directed Transfer Function (Kaminski and Blinowska, 1991), JPSTH – Joint Peri-Stimulus Time Histogram, MI – Mutual Information (Cover and Thomas, 2012), NC – Noise Correlations (Cohen and Kohn, 2011), PDC – Partial Directed Coherence (Baccalá and Sameshima, 2001), PPC – Pairwise Phase Consistency (Vinck et al., 2010), PSI – Phase Sloped Index (Nolte et al., 2004), RSEQ – statistical methods for detected Repeated SEquences of synchronous spiking (Torre et al., 2016; Russo and Durstewitz, 2017; Staude et al., 2010; Quaglio et al., 2017), SFC – Spike-Field Coherence, STAT – STATistical tools, STD – Spike-Train Dissimilarity measures, STTC – Spike Time Tiling Coefficient (Cutts and Eglén, 2014), WPL – Weighted Phase Lag index (Vinck et al., 2011).

Toolbox	(Cross)- corre- lation	Cohe- rence	Granger causality	Phase- amplitude coupling	Phase- locking value	Spike- triggered average	Spike- field cohe- rence	Unique features
Brainstorm	+	+	+	+	+	+	–	STAT
Chronux	–	+	–	–	–	+	+	STAT
Elephant	+	+	–	–	–	+	+	RSEQ, STD, STTC
FieldTrip	+	+	+	+	+	+	+	DTF, JPSTH, MI, NC, PDC, PPC, PSI, STAT, WPL
SPIKY	–	–	–	–	–	–	–	STD

349 - Chronux and FieldTrip compute confidence intervals for connectivity measures with jackknife re-
 350 sampling or variance estimates across trials, correspondingly (see Subsections 4.1-4.2); Brainstorm
 351 computes significance values for common connectivity measures, Elephant does not compute statistics
 352 on common connectivity measures.

353 To provide a better feeling of connectivity measures, we classify in Table 5 connectivity and synchro-
 354 nization measures mentioned in Table 4. We indicate for which signals the measure is applicable (Input),
 355 whether the measure is directed or not (Directed), is defined in time or frequency domain (Domain) and is bi-
 356 or multivariate (Dimension).

357 4.1 Comparing common tools: correlation, cross-correlation, coherence, Granger 358 causality, phase-amplitude coupling, phase-locking value, spike-field coherence 359 and spike-triggered average

360 In this subsection we compare implementations of common synchronization and connectivity measures
 361 for toolboxes from Table 4: correlation, cross-correlation, coherence, Granger causality, phase-amplitude
 362 coupling, phase-locking value, spike-field coherence and spike-triggered average.

363 Brainstorm and Elephant implement correlation, a pairwise non-directional time-domain connectivity
 364 measure. Brainstorm computes Pearson correlation coefficient (or optionally covariance) between spike trains
 365 and p-value of its significance; correlation is computed equivalently to MATLAB `corrcoef` function but in
 366 a faster vectorized way for $N > 2$ input signals. Elephant computes either Pearson correlation coefficient
 367 between binned spike trains (without additional statistics), pairwise covariances between binned spike trains
 368 (without additional statistics) or spike time tiling coefficient (STTC) introduced in (Cutts and Eglén, 2014).
 369 STTC, compared to correlation index introduced in (Wong et al., 1993), is described as not dependent on
 370 signals firing rate, correctly discriminating between lack of correlation and anti-correlation etc. (Cutts and
 371 Eglén, 2014). There is also a MATLAB STTC implementation⁴⁰.

⁴⁰<https://github.com/Leo-GG/NeuroFun/blob/master/%2Bcorrel/calcSTTC.m>

Table 5: Classification of synchronization and connectivity measures implemented in toolboxes listed in Table 4 regarding whether the measure is directed or not (Directed), is defined in time or frequency domain (Domain) and is bi- or multivariate (Dimension).

Measure	Directed	Domain	Dimension
Correlation and cross-correlation (CC)	–	Time	Bivariate
Coherence	–	Frequency	Bivariate
Directed transfer information (DTF)	+	Frequency	Multivariate
Granger causality (GC)	+	Time, frequency	Bivariate
Imaginary part of coherency (iCOH)	–	Frequency	Bivariate
ISI and SPIKE distance, SPIKE synchronization (STD)	–	Time	Bivariate
Joint peri-stimulus time histogram (JPSTH)	–	Time	Bivariate
Mutual information (MI)	–	Time	Bivariate
Noise correlation (NC)	–	Time	Bivariate
Phase amplitude coupling (PAC)	–	Frequency	Bivariate
Partial coherence (pCOH)	+	Frequency	Bivariate
Partial directed coherence (pdCOH)	+	Frequency	Multivariate
Phase-locking value (PLV)	–	Frequency	Bivariate
Pairwise phase consistency (PPC)	+	Frequency	Bivariate
Phase slope index (PSI)	+	Frequency	Bivariate
statistical methods for detecting Repeated SEquences of synchronous spiking (RSEQ)	–	Time	Multivariate
Spike field coherence (SFC)	–	Time	Bivariate
van Rossum and Viktor-Purpura spike train dissimilarity measures (STD)	–	Time	Bivariate
Spike time tiling coefficient (STTC)	–	Time	Bivariate
Weighted phase lag index (WPL)	–	Frequency	Bivariate

372 Cross-correlation is correlation between two signals computed for different time lags of one signal
 373 against the other. Elephant and FieldTrip implement cross-correlation, a pairwise non-directional time-
 374 domain connectivity measure. Between two binned spike trains Elephant computes cross-correlation for
 375 user-defined window with optional correction of border effect, kernel smoothing (for boxcar, Hamming,
 376 Hanning and Bartlett) and normalization. Between two LFP signals Elephant computes the standard unbiased
 377 estimator of the cross-correlation function (Stoica et al., 2005, Eq. 2.2.3) for user-defined time-lags without
 378 additional statistics across trials; note that biased estimator of the cross-correlation function is more accurate
 379 as discussed in (Stoica et al., 2005). FieldTrip computes cross-correlation between two spike channels for
 380 user-defined time lags and bin size (correlogram can optionally be debiased depending on data segment
 381 length). FieldTrip computes shuffled and unshuffled correlograms: if two channels are independent, the
 382 shuffled cross-correlogram should be the same as unshuffled.

383 Brainstorm, Chronux, Elephant and FieldTrip implement coherence, a frequency-domain equivalent of
 384 cross-correlation (Bastos and Schoffelen, 2016):

385 - Brainstorm implements coherence according to (Carter, 1987) computing also p-values of parametric
 386 significance estimation;

387 - Chronux computes coherence between two (binned) point-processes or LFP signals using multitaper
 388 method, with confidence intervals or jackknife resampled error bars;

389 - Elephant computes coherence using Welch's method with phase lags but without additional statistics.
 390 Computing coherence across trials is not supported in the considered version;

391 - FieldTrip computes coherence according to (Rosenberg et al., 1989) with variance estimate across

392 trials. Additionally, FieldTrip provides computing of partial coherence according to (Rosenberg et al.,
 393 1998), partial directed coherence (Baccalá and Sameshima, 2001) and imaginary part of coherency
 394 (Nolte et al., 2004) with variance across trials. Partial directed coherence (PDC) is a directional
 395 measure. Compared to coherence, PDC is shown to reflect a frequency-domain representation of the
 396 concept of Granger causality (Baccalá and Sameshima, 2001).

397 Elephant does not provide built-in tools to compare coherence values between two conditions, Chronux
 398 provides a two-group test, FieldTrip provides an independent samples Z-statistic via `ft_freqstatistics`
 399 function by the method described in (Maris et al., 2007), Brainstorm is using FieldTrip `ft_freqstatistics`
 400 function.

401 Brainstorm and FieldTrip implement Geweke's extension of the original time-domain concept of Granger
 402 causality (GC) introduced in (Granger, 1969) to the frequency domain (Geweke, 1982). GC implemented in
 403 Brainstorm and FieldTrip is a frequency-domain pairwise directional measure of connectivity. FieldTrip
 404 GC implementation is based on (Brovelli et al., 2004). The multivariate autoregressive (MVAR) model in
 405 FieldTrip uses biosig or BSMART toolboxes implementation on user choice, which are included in FieldTrip.
 406 FieldTrip computes variance of GC values across trials. Neither Brainstorm nor FieldTrip provide built-in
 407 tools/prescribed procedure to statistically compare GC values between conditions. Different to FieldTrip,
 408 Brainstorm computes as well time-resolved GC between two signals using two Wald statistics according
 409 to (Geweke, 1982) and (Hafner and Herwartz, 2008). The directed transfer function and partial directed
 410 coherence are multivariate extensions of Granger causality (Blinowska, 2011).

411 In Figure 6 we compare values of several connectivity measures computed in Brainstorm, Chronux and
 412 FieldTrip for simulated data with autoregressive models⁴¹ according to Eq. (5) (computing coherence across
 413 trials is not included in the considered Elephant version).

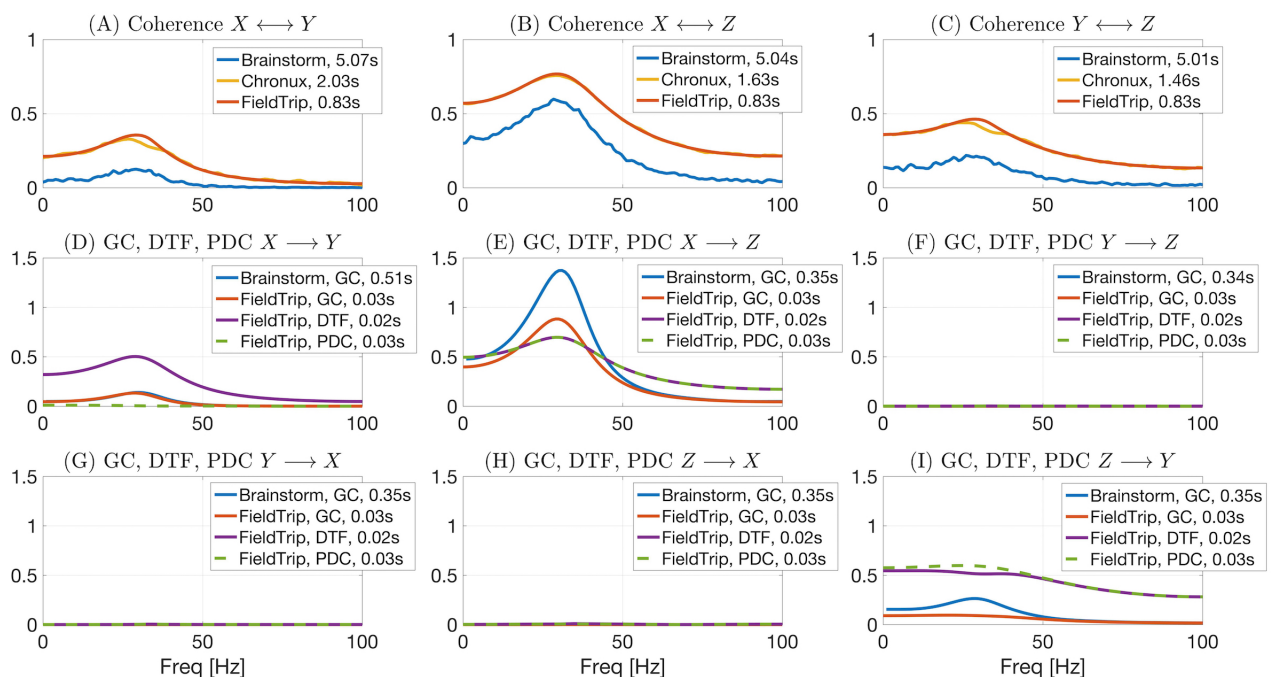


Figure 6: Comparing Brainstorm, Chronux and FieldTrip implementations of connectivity measures for signals simulated by autoregressive models (see Eq. (5)). While coherence is non-directional, Granger Causality (GC), Directed Transfer Function (DTF, see Subsection 4.2 for more details) and Partial directed Coherence (PDC) are directional measures. PDC allows to correctly detect interaction between signals (no direct $X \rightarrow Y$ interaction). Chronux and FieldTrip provide faster implementations compared to Brainstorm (see computing times in plots legends) and return variance across trials. Brainstorm coherence values are noisier since there Welch method is used in contrast to multitapers (Chronux) or multivariate autoregressive modeling (FieldTrip).

⁴¹<http://www.fieldtriptoolbox.org/tutorial/connectivity/>

$$\begin{aligned}x(t) &= 0.8x(t-1) - 0.5x(t-2), \\y(t) &= 0.9y(t-1) + 0.5z(t-1) - 0.8y(t-2), \\z(t) &= 0.5z(t-1) + 0.4x(t-1) - 0.2z(t-2).\end{aligned}\tag{5}$$

414 Brainstorm and FieldTrip implement phase-amplitude coupling (PAC), a frequency-domain pairwise
415 non-directional measure (Canolty et al., 2006; Samiee and Baillet, 2017; Voytek et al., 2010). FieldTrip
416 implements two types of PAC⁴²: mean vector length and modulation index according to (Tort et al., 2010).
417 Brainstorm implements PAC according to (Özkurt and Schnitzler, 2011). Both Brainstorm and FieldTrip do
418 not compute additional statistics on PAC.

419 Brainstorm and FieldTrip implement phase-locking value (PLV), a frequency-domain pairwise non-
420 directional measure (Lachaux et al., 1999). PLV checks how consistent the phase relation between the two
421 signals is across trials. We refer to (Vinck et al., 2011; Bastos and Schoffelen, 2016) for a comparison of
422 different phase synchronization metrics and their biases. FieldTrip computes PLV based on (Lachaux et al.,
423 1999) with a variance estimate using jackknife resampling.

424 Combination of spiking activity and LFP is often used to study rhythmic neuronal synchronization
425 since spike-LFP measures are more sensitive than spike-spike synchronization measures (Vinck et al., 2012;
426 Chakrabarti et al., 2014). To this end Brainstorm, Chronux, FieldTrip and Elephant implement a spike-field
427 coherence (SFC), a frequency-domain pairwise non-directional measure. Brainstorm implements SFC
428 according to (Fries et al., 2001) for user-defined window size around spikes without additional statistics
429 computed. Chronux implements SFC with a multitaper approach for user-defined tapers and frequency band,
430 computing also a confidence level of coherency and jackknife or standard error bars. FieldTrip computes
431 SFC with variance across trials (see details in the corresponding tutorial⁴³). Elephant implements SFC using
432 standard Python `scipy.signal.coherence()` function, no additional statistics is computed.

433 One of the first steps in the analysis of spike-field coupling is computing of a spike-triggered average
434 (STA) of LFP that is an average LFP voltage within a small window of the time around every spike. While
435 neither Brainstorm nor Elephant compute any additional statistic on STA, Chronux computes STA with an
436 optional kernel smoothing and calculates bootstrapped standard error on computed values and FieldTrip
437 computes mean and variance of STA values.

438 4.2 Description of unique tools

439 In this subsection we describe unique tools of the toolboxes from Table 4. Elephant provides five recent
440 statistical tools to study higher-order correlations and synchronous spiking events in parallel spike trains:

- 441 - ASSET (Analysis of Synchronous Spike Events) implements the method from (Torre et al., 2016)
442 and is an extension of the visualization method from (Schrader et al., 2008). ASSET assesses the
443 statistical significance of simultaneous spike events (SSE) and aims to detect such events that cannot
444 be explained on the basis of rate coding mechanisms and arise from spike correlations on shorter time
445 scale;
- 446 - CAD (Cell Assembly Detection) implements the method from (Russo and Durstewitz, 2017) for
447 capturing structures of higher-order correlations in massively parallel spike train recordings with
448 arbitrary time lags and at multiple time-scale; CAD makes statistical parametric testing between each
449 pair of neurons followed by an agglomerative recursive algorithm aiming to detect statistically precise
450 repetitions of spikes in the data;

⁴²http://www.fieldtriptoolbox.org/reference/ft_crossfrequencyanalysis/

⁴³<http://www.fieldtriptoolbox.org/tutorial/spikefield/>

- 451 - CuBIC (Cumulant Based Inference of higher order Correlations) implements a statistical method
452 (Staude et al., 2010) for detecting higher order correlations in parallel spike train recordings;
- 453 - SPADE (Spike Pattern Detection and Evaluation) implements the method from (Quaglio et al., 2017)
454 for assessing the statistical significance of repeated occurrences of spike sequences (spatio-temporal
455 patterns) based on recent methods in (Torre et al., 2013; Quaglio et al., 2017). SPADE aims to
456 overcome computational and statistical limits in detecting repeated spatio-temporal patterns within
457 massively parallel spike trains (Quaglio et al., 2017), see (Quaglio et al., 2018) for a recent review of
458 methods for identification of spike patterns in massively parallel spike trains;
- 459 - UE (Unitary Event analysis) implements the statistical method from (Grün et al., 1999, 2002) for
460 analyzing excess spike correlations between simultaneously recorded neurons. This method compares
461 the empirical spike coincidences to the expected number on the basis of firing rate of the neurons.
- 462 Elephant and SPIKY toolboxes allow to compute measures of spike train dissimilarity (also referred as
463 measures of spike train synchrony). Elephant implements well-known time-scale dependent van Rossum
464 (van Rossum, 2001) and (Victor and Purpura, 1996) dissimilarity distances whereas SPIKY implements three
465 recent parameter-free time-scale independent measures: ISI-distance (Kreuz et al., 2007), SPIKY distance
466 (Kreuz et al., 2012) and SPIKE synchronization (Quiroga et al., 2002). We refer to (Chicharro et al., 2011;
467 Kreuz et al., 2012; Mulansky et al., 2015) for a comparison of dissimilarity measures. Note also MATLAB
468 implementations of dissimilarity measures at J.D. Victor⁴⁴ and T. Kreuz⁴⁵ web-sites.
- 469 FieldTrip, compared to other toolboxes from Table 4, computes and visualizes⁴⁶ the following classic
470 and recent connectivity and synchronization measures:
- 471 - directed transfer function (DTF) introduced in (Kaminski and Blinowska, 1991) is a multivariate
472 frequency-domain directional connectivity measure; FieldTrip computes it according to (Kaminski
473 and Blinowska, 1991) from cross-spectral density with a variance across trials. DTF, compared to GC,
474 makes a multivariate spectral decomposition, the advantage of this approach is that interaction between
475 all channels is taken into account (see, e.g., Figure 6 in Subsection 4.1). However pairwise measures
476 yield more stable results since they involve fitting fewer parameters (Blinowska, 2011; Bastos and
477 Schoffelen, 2016);
- 478 - joint peri-stimulus time histogram (JPSTH) is a pairwise time-domain non-directional measure between
479 spike trains that allows to gain insight into temporal evolution of spike-spike correlations (Brown
480 et al., 2004; Aertsen et al., 1987). To check whether the resulted JPSTH is caused by task-induced
481 fluctuations of firing rate or by temporal coordination not time-locked to stimulus onset, FieldTrip also
482 computes JPSTH with shuffling subsequent trials. We illustrate JPSTH visualization with FieldTrip
483 tools in Figure 7;
- 484 - mutual information (MI) is a pairwise time-domain non-directional connectivity measure. FieldTrip
485 computes MI using implementation from ibtb toolbox (Magri et al., 2009) without additional statistics;
- 486 - noise correlations (NC) is a non-directional pairwise time-domain measure that can be computed
487 between two spike trains; NC measures whether neurons share trial-by-trial fluctuations in their firing
488 rate; different to so called signal correlations (SC), these fluctuations are measured over repetitions of
489 identical experimental conditions, i.e. are not driven by variable sensory or behaviorally conditions;
- 490 - phase-coupling pairwise spike-field measures compute the phases of spikes relative to the ongoing
491 LFP with a discrete Fourier transform of an LFP segment around the spike time (Vinck et al., 2012).
492 FieldTrip implements recent methods from (Vinck et al., 2012): angular mean of spike phases, Rayleigh

⁴⁴<http://www-users.med.cornell.edu/~jdvicto/pubalgor.html>

⁴⁵<http://wwwold.fi.isc.cnr.it/users/thomas.kreuz/Source-Code/VanRossum.html>

⁴⁶http://www.fieldtriptoolbox.org/reference/ft_connectivityplot/

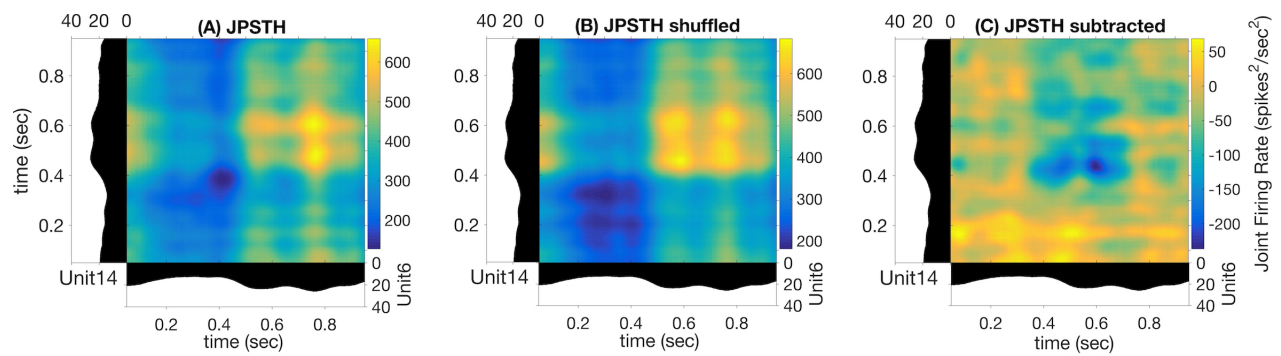


Figure 7: Illustration of FieldTrip functionality: joint peri-stimulus time histogram (JPSTH) (A), shuffled JPSTH (B) and their difference (C) for test dataset between M1 units 6 and 42, monkey MM (colorbar values range is different for each subplot, this range is not adjustable outside of FieldTrip).

493 p-value and pairwise-phase consistency according to the method in (Vinck et al., 2010). We refer to
494 (Vinck et al., 2010; Bastos and Schoffelen, 2016) for a discussion and comparison of these measures;

495 - phase-slope index (PSI) is a directional pairwise frequency-domain measure that can be computed
496 between two signals from their complex-valued coherency. FieldTrip computes PSI according to
497 (Nolte et al., 2008) with variance across trials;

498 - pairwise phase consistency (PPC) is a directional pairwise frequency-domain measure that can be
499 computed from the distribution of pairwise differences of the relative phases. PPC compared to PLV is
500 not biased by sample size (Bastos and Schoffelen, 2016). FieldTrip computes PPC with leave-one-out
501 variance estimate;

502 - weighted phase-lag index (WPL) introduced in (Vinck et al., 2011) is a non-directional pairwise
503 frequency-domain measure computed from cross-spectral density between two signals. WPL was
504 introduced to solve the problem with sensitivity of phase-lag index (Stam et al., 2007) to volume-
505 conduction and noise (Vinck et al., 2011). FieldTrip computes WPL according to (Vinck et al., 2011)
506 with variance across trials.

507 **5 SPECIALIZED TOOLBOXES FOR DIMENSIONALITY REDUCTION AND GENER-** 508 **ALIZED LINEAR MODELING**

509 In this section we overview specialized toolboxes for dimensionality reduction (Subsection 5.1) and general-
510 ized linear modeling (Subsection 5.2). Compared to Table 1, we do not provide in the corresponding tables
511 for specialized toolboxes information on

512 - Import/Export since none of the considered toolboxes supports importing/exporting from specialized
513 spike data formats;

514 - GUI since only DataHigh toolbox provides GUI (see details below).

515 **5.1 Toolboxes for dimensionality reduction**

516 Dimensionality reduction of neural data allows to obtain a simplified low-dimensional representation of
517 neural activity. In Table 6 we compare open-source toolboxes for dimensionality reduction of neural data
518 (note also a list of dimensionality reduction software actively updating at B. Yu web-site⁴⁷). See examples
519 for application of DataHigh, dPCA and TCA toolboxes in our open MATLAB script.

⁴⁷<http://users.ece.cmu.edu/~byronyu/software.shtml>

Table 6: Features of open-source dimensionality reduction toolboxes regarding visualization tools, principal and usage programming language, availability of documentation, number of citations, and support by updates at least once per year. ccpTD – coupled canonical polyadic Tensor Decomposition, DCA – Distance Covariances Analysis, (GP)FA – (Gaussian Process) Factor Analysis, LDA – Fisher’s Linear Discriminant Analysis, NMF – Non-negative Matrix Factorization, (d,p)PCA – (demixed, probabilistic) Principal Component Analysis, (nn)TCA – (non-negative) Tensor Component Analysis

Toolbox, version	Visuali- zation	Language	Documen- tation	Cited	Support	Methods
DataHigh v.1.2	+	MATLAB	+	<30	In part	FA, GPFA, LDA, PCA
DCA v1.0	–	MATLAB	In part	<30	In part	DCA
dPCA v0.1	+	Python MATLAB	+	<300	+	dPCA, PCA
GPFA v.2.03	+	MATLAB	In part	>300	In part	FA, PCA, pPCA, GPFA
seqNMF	+	MATLAB	+	<30	+	NMF, PCA
tensor-demo	+	Python MATLAB	+	<30	+	TCA
tensortools v0.3.0	+	Python	+	<30	+	ccpTD, nnTCA
TD-GPFA v3.0	+	MATLAB	In part	<30	In part	FA, GPFA, PCA, pPCA

520 We have indicated “In part” in Documentation column for GPFA and TD-GPFA toolboxes since they
 521 provide usage examples and readme files with notes on parameters choice but but neither detailed manual
 522 nor tutorial, they refer to the original publication (Yu et al., 2009) for details. We have indicated “In part” in
 523 Documentation column for DCA tool since it provides neither manual nor tutorial (only example of use in
 524 MATLAB script comments). DataHigh and GPFA toolboxes are not uploaded to GitHub or any other public
 525 version control system preventing from tracking version changes and submitting bugs. DCA and TD-GPFA
 526 toolboxes have not been updated during the last 2 years.

527 Compared to other toolboxes from Table 6,

528 - DataHigh provides a user-friendly GUI illustrating algorithm steps such as choice of bin size, smooth-
 529 ing, components number etc.;

530 - dPCA is applied on trial-averaged spiking activity; dPCA breaks down the neural activity into
 531 components each of which relates to time (condition-independent component) or a single experimental
 532 condition of the task; the idea is an easier task-relevant interpretation compared to the standard PCA
 533 or ICA; the results can be summarized in a single figure (Kobak et al., 2016);

534 - TD-GPFA allows to extract low-dimensional latent structure from time series in the presence of delays;

535 - tensor-demo and tensortools allow to reduce dimensionality both across and within trials (Williams
 536 et al., 2018).

537 In Table 7 we outline additional dimensionality reduction tools provided by the toolboxes.

538 It is important to check whether input data fit model assumptions when applying dimensionality reduction
 539 methods: whether the data are allowed to be non-stationary, contain outliers, observational noise or be
 540 correlated, whether recorded activity evolves in a low-dimensional manifold, which sample size is sufficient
 541 etc. Discussing model assumptions for each of dimensionality reduction methods is beyond the scope of
 542 this paper, we refer to the original papers and to the model assumptions for applying principal component
 543 analysis (PCA) formulated in (Shlens, 2014).

Table 7: Comparing dimensionality reduction toolboxes: diagnostic and statistical tools. In Statistical tests column we indicate whether the toolbox provides possibility to measure significance of results and provides permutation or re-shuffling tests on the data.

Toolbox	Cross-validation	Tool to select optimal dimensions number	Fitting error, variance explained	Statistical tests
DataHigh	+	+	+	-
DCA	-	-	-	-
dPCA	+	+	+	+
GPFA	+	+	+	-
seqNMF	+	+	+	+
tensor-demo	-	+	+	-
tensortools	-	+	+	+
TD-GPFA	+	+	+	-

544 5.2 Toolboxes for GLM analysis

545 Generalized linear models (GLMs) are often applied for predicting spike counts with the aim to understand
 546 which factors influence simultaneous spiking activity: whether it is predicted by the past or concurrent
 547 neural activity of the same or remote brain area or by external covariates. In Table 8 we overview major
 548 open-source toolboxes for GLM analysis. These toolboxes do not contain any general spike data analysis
 549 functions besides GLM analysis since they are either GLM tutorials or codes related to particular analysis
 550 made in the paper.

Table 8: Features of open-source toolboxes for generalized linear modeling of spike data regarding visualization tools, principal and usage programming language, availability of documentation, number of citations (for the paper with the introduced method), support by updates at least once per year and implemented methods. cGLM – GLM with coupling filters, gGLM – linear Gaussian GLM, GNM – Generalized Nonlinear Model (Butts et al., 2011), GQM – Generalized Quadratic Model (Park and Pillow, 2011), pGLM – Poisson GLM (Truccolo et al., 2005), ppGLM – point-process GLM (Paninski et al., 2007), NIM – Nonlinear Input Model (McFarland et al., 2013), SHF – Spikes and covariates History Filters, STB – Smooth Temporal Basis

Toolbox, version	Methods	Visuali- zation	Language	Documen- tation	Cited	Support
Case-Studies	pGLM	+	MATLAB	+	<30	+
GLMcode1	pGLM	+	MATLAB	+	<30	-
GLMcode2	pGLM	+	MATLAB	+	<30	-
GLMspiketools v1	cGLM, pGLM, SHF, STB	+	MATLAB	+	>900	+
GLMspike- traintutorial	cGLM, gGLM, pGLM, SHF	+	MATLAB	+	>900	+
neuroGLM	pGLM, SHF, STB	+	MATLAB	+	>90	+
NIMclass v1.0	GLM, GQM, GNM, NIM	-	MATLAB	-	>90	+
nStat v2	ppGLM	+	MATLAB	In part	<30	+
spykesML v0.1.dev	pGLM, SHF	-	Python	+	<30	+

551 GLMcode1 and GLMcode2 codes are not uploaded to GitHub or any other version control system as they
 552 implement methods for particular analysis made in the papers (see below) are not supposed to be updated.
 553 Note that

- 554 - Case-Studies implements (see folders Chapter 9, 10, 11 on GitHub⁴⁸) basic steps of Poisson GLM
555 fitting with history dependence to the data on sample datasets for the corresponding book (Kramer and
556 Eden, 2016);
- 557 - GLMcode1, GLMcode2 implement the code for the papers (Glaser et al., 2018) and (Lawlor et al.,
558 2018);
- 559 - examples of use for nStat toolbox are located in helpfiles folder in the corresponding GitHub
560 repository;
- 561 - spykesML tool provides comparison of GLM performance with several methods from modern machine
562 learning approaches (including neural networks);
- 563 - NIMclass uses MATLAB optimization toolbox and contains many examples for real-world data;
- 564 - GLMspiketutorial is a tutorial for teaching purposes. It is not memory-efficient implemented,
565 but it makes easy to understand the basic steps of Poisson and Gaussian GLMs fitting, analysis and
566 comparison for spike data ⁴⁹. neuroGLM and GLMspiketools are more advanced tools with efficient
567 memory implementation. Additionally to GLMspiketutorial, they support some advanced GLM
568 features such as smooth temporal basis functions for spike-history filters, different time-scales for
569 stimulus and spike-history components etc.

570 6 CONCLUSIONS

571 In this review we have compared major open-source toolboxes for spike and local field potentials (LFP)
572 processing and analysis. We have compared toolboxes functionality, statistical and visualization tools,
573 documentation and support quality. Besides summarizing information about toolboxes in comparison tables,
574 we have discussed and illustrated particular toolboxes functionality and implementations, also in our open
575 MATLAB code. Below we summarize the comparisons that we made for general spike and LFP analysis
576 toolboxes and toolboxes with connectivity tools.

577 Each considered toolbox has its own advantages:

- 578 - Brainstorm: graphical user interface (GUI), versatile and cross-checked functionality (highly-cited),
579 statistical tools, detailed tutorials with recommendations on parameters choice, support of many
580 file formats, active user discussion community and regular hands-on sessions, fast Morlet wavelet
581 transform implementation;
- 582 - Chronux: versatile and cross-checked functionality (highly-cited), statistical tools (measures of
583 variance across trials and statistical comparing between different conditions), detailed documentation,
584 convenient data analysis pipeline for programming-oriented users (detailed code comments and
585 modular code design);
- 586 - Elephant: support of many file formats, versatile functionality with implementation of classic and
587 recent methods for spike-spike connectivity and synchronization analysis, fast Morlet wavelet transform
588 implementation;
- 589 - FieldTrip: versatile and cross-checked functionality (highly-cited), statistical tools (measures of
590 variance across trials and statistical comparing between different conditions), detailed tutorials with
591 recommendations on parameters choice, support of many file formats, active user discussion community
592 and regular hands-on sessions, flexible visualization tools, convenient data analysis pipeline for
593 programming-oriented users (detailed code comments and modular code design), versatile filtering,
594 connectivity and synchronization analysis tools, fast and accurate line noise removal;

⁴⁸<https://github.com/Mark-Kramer/Case-Studies-Kramer-Eden>

⁴⁹<https://github.com/pillowlab/GLMspiketutorial>

- 595 - gramm: quick publication-quality PSTH, raster plots and tuning curves with many easily adjustable
596 plot properties;
- 597 - Spike Viewer: GUI, support of many file formats;
- 598 - SPIKY: GUI, implementation of recent spike train dissimilarity measures.

599 **7 LIST OF TOOLBOXES AND TOOLS IN ALPHABETICAL ORDER WITH LINKS**

600 Below all the considered toolboxes are provided with a brief description, reference to the paper where the
601 toolbox was introduced and a link for downloading.

- 602 - Brainstorm^{50,51} (Tadel et al., 2011) – a MATLAB toolbox for the analysis of brain recordings: MEG,
603 EEG, fNIRS, ECoG, depth electrodes and animal invasive neurophysiology;
- 604 - BSMART⁵² (Brain-System for Multivariate AutoRegressive Time series) (Cui et al., 2008) – a
605 MATLAB/C toolbox for spectral analysis of continuous neural data recorded from several sensors;
- 606 - Case-Studies⁵³ – a MATLAB set of examples on sample datasets accompanying the corresponding
607 book (Kramer and Eden, 2016);
- 608 - Chronux⁵⁴ (Bokil et al., 2010) – a MATLAB package for the analysis of neural data;
- 609 - DataHigh⁵⁵ (Cowley et al., 2013) – a MATLAB-based graphical user interface to visualize and interact
610 with high-dimensional neural population activity;
- 611 - DATA-MEAns⁵⁶ (Bonomini et al., 2005) – a Delphi7 tool for the classification and management of
612 neural ensemble recordings;
- 613 - DCA⁵⁷ (Cowley et al., 2017) (distance covariance analysis) – an implementation (MATLAB and
614 Python) of the linear dimensionality reduction method that can identify linear and nonlinear relationships
615 between multiple datasets;
- 616 - dPCA⁵⁸ (demixed Principal Component Analysis) (Kobak et al., 2016) – a MATLAB implementation
617 of the linear dimensionality reduction technique that automatically discovers and highlights the
618 essential features of complex population activities;
- 619 - Elephant^{59,60} (Yegenoglu et al., 2017) – an Electrophysiology Analysis Toolkit in Python. Elephant
620 toolbox includes functionality from earlier developed toolboxes CSDPlotter⁶¹ (Pettersen et al., 2006)
621 and iCSD 2D⁶², it is a direct successor of NeuroTools;

⁵⁰<https://neuroimage.usc.edu/brainstorm/Introduction>

⁵¹<https://github.com/brainstorm-tools/brainstorm3>

⁵²<http://www.brain-smart.org>

⁵³<https://github.com/Mark-Kramer/Case-Studies-Kramer-Eden>

⁵⁴<http://chronux.org>

⁵⁵<http://users.ece.cmu.edu/~byronyu/software/DataHigh/datahigh.html>

⁵⁶<http://cortivis.umh.es>

⁵⁷<https://github.com/BenjoCowley/dca>

⁵⁸<https://github.com/machenslab/dPCA>

⁵⁹<http://neuralensemble.org/elephant/>

⁶⁰<https://github.com/NeuralEnsemble/elephant/commits/master>

⁶¹<https://github.com/espenhgn/CSDplotter>

⁶²<http://www.neuroinf.pl/Members/szleski/csd2d/toolbox>

- 622 - FieldTrip^{63,64} (Oostenveld et al., 2011) – a MATLAB toolbox for advanced analysis of MEG, EEG,
623 and invasive electrophysiological (spike and LFP) data;
- 624 - FIND⁶⁵ (Meier et al., 2008) – a MATLAB toolbox for the analysis of neuronal activity;
- 625 - GLMcode1 – a MATLAB code implementing data analysis for particular publication (Glaser et al.,
626 2018) with GLM fitting to analyze factors contributing to neural activity (this code is available from
627 the authors upon request);
- 628 - GLMcode2⁶⁶ (Perich et al., 2018) – a MATLAB code implementing data analysis for particular
629 publication (Lawlor et al., 2018) with GLM fitting to estimate preferred direction for each neuron;
- 630 - GLMspikestools⁶⁷ (Pillow et al., 2008) – a Generalized Linear Modeling tool for single and multi-
631 neuron spike trains;
- 632 - GLMspiketrainutorial⁶⁸ (Pillow et al., 2008) – a simple tutorial on Gaussian and Poisson GLMs for
633 single and multi-neuron spike train data;
- 634 - GPFA⁶⁹ (Gaussian-Process Factor Analysis) (Yu et al., 2009) – a MATLAB implementation of the
635 method extracting low-dimensional latent trajectories from noisy, high-dimensional time series data. It
636 combines linear dimensionality reduction (factor analysis) with Gaussian-process temporal smoothing
637 in a unified probabilistic framework;
- 638 - gramm^{70,71} (Morel, 2018) – a plotting MATLAB toolbox for quick creation of complex publication-
639 quality figures;
- 640 - HERMES⁷² (Niso et al., 2013) – a MATLAB toolbox for assessing connectivity and synchronization
641 between time series;
- 642 - ibTB⁷³ (Information Breakdown Toolbox) (Magri et al., 2009) – a C/MATLAB toolbox for fast
643 information analysis of multiple-site LFP, EEG and spike train recordings;
- 644 - Inform⁷⁴ (Moore et al., 2017) – a cross-platform C library for information analysis of dynamical
645 systems;
- 646 - infoToolbox⁷⁵ (Magri et al., 2009) – a toolbox for the fast analysis of multiple-site LFP, EEG and
647 spike train recordings;
- 648 - JIDT⁷⁶ (Lizier, 2014) – an information-theoretic Java toolbox for studying dynamics of complex
649 systems;

⁶³<http://www.fieldtriptoolbox.org>

⁶⁴<https://github.com/fieldtrip/fieldtrip>

⁶⁵<http://find.bccn.uni-freiburg.de>

⁶⁶<https://crcns.org/data-sets/motor-cortex/pmd-1/about-pmd-1>

⁶⁷http://pillowlab.princeton.edu/code_GLM.html

⁶⁸<https://github.com/pillowlab/GLMspiketrainutorial>

⁶⁹<http://users.ece.cmu.edu/~byronyu/software.shtml>

⁷⁰<https://www.mathworks.com/MATLABcentral/fileexchange/54465-gramm-complete-data-visualization-toolbox-ggplot2-r-like>

⁷¹<https://github.com/piermorel/gramm>

⁷²<http://hermes.ctb.upm.es>

⁷³<http://www.ibtb.org>

⁷⁴<https://github.com/ELIFE-ASU/Inform>

⁷⁵<http://www.infotoolbox.org>

⁷⁶<https://github.com/jlizier/jidt>

- 650 - MEAbench⁷⁷ (Wagenaar et al., 2005) – a C++ toolbox for multi-electrode data acquisition and online
651 analysis;
- 652 - MEA-tools⁷⁸ (Egert et al., 2002) – a collection of MATLAB-based tools to analyze spike and LFP
653 data from extracellular recordings with multi-electrode arrays;
- 654 - MuTe⁷⁹ (Montalto et al., 2014) – a MATLAB toolbox to compare established and novel estimators of
655 the multivariate transfer entropy;
- 656 - MVGC⁸⁰ (Multivariate Granger Causality MATLAB Toolbox) (Barnett and Seth, 2014) – a MATLAB
657 toolbox facilitating Granger-causal analysis with multivariate multi-trial time series data;
- 658 - neuroGLM⁸¹ (Park et al., 2014) – an MATLAB tool, an extension of GLMspiketrain tutorial allow-
659 ing more advanced features of GLM modeling such as smooth basis functions for spike-history
660 filters, memory-efficient temporal convolutions, different timescales for stimulus and spike-history
661 components, low-rank parametrization of spatio-temporal filters, flexible handling of trial-based data;
- 662 - NIMclass^{82,83} (McFarland et al., 2013) – a MATLAB implementation of the nonlinear input model. In
663 this model, the predicted firing rate is given as a sum over nonlinear inputs followed by a “spiking
664 nonlinearity” function;
- 665 - nStat⁸⁴ (neural Spike Train Analysis Toolbox) (Cajigas et al., 2012) – an object-oriented MATLAB
666 toolbox that implements several models and algorithms for neural spike train analysis;
- 667 - OpenElectrophy^{85,86} (Garcia and Fourcaud-Trocmé, 2009) – a Python framework for analysis of intro-
668 and extra-cellular recordings;
- 669 - PyEntropy⁸⁷ (Ince et al., 2009) – a Python module for estimating entropy and information theoretic
670 quantities using a range of bias correction methods;
- 671 - seqNMF⁸⁸ (Mackevicius et al., 2019) – a MATLAB toolbox for unsupervised discovery of temporal
672 sequences in high-dimensional datasets with applications to neuroscience;
- 673 - SIFT⁸⁹ (Delorme et al., 2011; Mullen, 2014) – a Source Information Flow MATLAB EEGLAB-
674 compatible toolbox for analysis and visualization of multivariate causality and information flow
675 between sources of electrophysiological (EEG/ECOG/MEG) activity;
- 676 - SigMate⁹⁰ (Mahmud et al., 2012) – a MATLAB toolbox for extracellular neuronal signal analysis;
- 677 - sigTOOL⁹¹ (Lidierth, 2009) – a MATLAB toolbox for spike data analysis;

⁷⁷<http://www.danielwagenaar.net/meabench.html>

⁷⁸<http://material.brainworks.uni-freiburg.de/research/meatools/>

⁷⁹https://figshare.com/articles/MuTE_toolbox_to_evaluate_Multivariate_Transfer_Entropy/1005245

⁸⁰<http://www.sussex.ac.uk/sackler/mvdc/>

⁸¹<https://github.com/pillowlab/neuroGLM>

⁸²<http://neurotheory.umd.edu/nimcode>

⁸³<https://github.com/dbutts/NIMclass>

⁸⁴<https://github.com/iahncajigas/nSTAT>

⁸⁵<http://neuralensemble.org/OpenElectrophy/>

⁸⁶<https://github.com/OpenElectrophy/OpenElectrophy>

⁸⁷<https://github.com/robince/pyentropy>

⁸⁸<https://github.com/FeeLab/seqNMF>

⁸⁹<https://sccn.ucsd.edu/wiki/SIFT>

⁹⁰<https://sites.google.com/site/muftimahmud/codes>

⁹¹<http://sigtool.sourceforge.net/>

- 678 - Spike Viewer⁹² (Pröpper and Obermayer, 2013) – a multi-platform GUI application for navigating,
679 analyzing and visualizing electrophysiological datasets;
- 680 - SPIKY^{93,94} (Kreuz et al., 2015) – a MATLAB graphical user interface that facilitates application of
681 time-resolved measures of spike-train synchrony to both simulated and real data;
- 682 - SPKTool⁹⁵ (Liu et al., 2011) – a MATLAB toolbox for spikes detection, sorting and analysis;
- 683 - spykesML⁹⁶ (Benjamin et al., 2018) – a Python toolbox with a tutorial for comparing performance of
684 GLM with modern machine-learning methods (neural networks, random forest etc.);
- 685 - STAR⁹⁷ (Spike Train Analysis with R) (Pouzat and Chaffiol, 2009) – an R package to analyze spike
686 trains;
- 687 - STAToolkit⁹⁸ (Spike Train Analysis Toolkit) (Goldberg et al., 2009) – a MATLAB package for the
688 information theoretic analysis of spike train data;
- 689 - tensor-demo⁹⁹ – a MATLAB and Python package (available for both languages) for fitting and
690 visualizing canonical polyadic tensor decompositions of higher-order data arrays;
- 691 - tensortools¹⁰⁰ – a Python package for fitting and visualizing canonical polyadic tensor decompositions
692 of higher-order data arrays;
- 693 - TD-GPFA¹⁰¹ (time-delayed Gaussian-Process Factor Analysis) (Lakshmanan et al., 2015) – a MAT-
694 LAB implementation of GPFA method extension that allows for a time delay between each latent
695 variable and each neuron;
- 696 - ToolConnect¹⁰² (Pastore et al., 2016) – a functional connectivity C# toolbox with GUI for in vitro
697 networks;
- 698 - Trentool¹⁰³ (Lindner et al., 2011) – a MATLAB toolbox for the analysis of information transfer in
699 time series data. Trentool provides user friendly routines for the estimation and statistical testing of
700 transfer entropy in time series data.

701 CONFLICT OF INTEREST STATEMENT

702 The authors have declared that no competing interests exist.

703 AUTHOR CONTRIBUTIONS

704 VU performed the reported study. VU wrote and AG edited the paper. Both authors have seen and approved
705 the final manuscript.

⁹²<https://github.com/rproepp/spykeviewer>

⁹³<https://github.com/mariomulansky/PySpike>

⁹⁴<http://wwwold.fi.isc.cnr.it/users/thomas.kreuz/Source-Code/SPIKY.html>

⁹⁵<https://sourceforge.net/projects/spktool/files/latest/download>

⁹⁶<https://github.com/KordingLab/spykesML>

⁹⁷<https://sites.google.com/site/spiketrainanalysiswithr/>

⁹⁸<https://omictools.com/statoolkit-tool>

⁹⁹<https://github.com/ahwillia/tensor-demo>

¹⁰⁰<https://github.com/ahwillia/tensortools>

¹⁰¹<https://github.com/karts25/NeuralTraj>

¹⁰²<http://software.incf.org/software/toolconnect>

¹⁰³<https://trentool.github.io/TRENTOOL3/>

706 FUNDING

707 The work was supported by grants of the Deutsche Forschungsgemeinschaft through the Collaborative
708 Research Center 889 “Cellular Mechanisms of Sensory Processing” and the Research Unit 1847 “The
709 Physiology of Distributed Computing Underlying Higher Brain Functions in Non-Human Primates”, and by
710 the European Commission through the H2020 project Plan4Act (FETPROACT-16 732266), all granted to
711 AG. The funder had no role in study design, data collection and analysis, decision to publish, or preparation
712 of the manuscript.

713 DATA AVAILABILITY STATEMENT

714 The datasets analyzed and generated for this study can be found at (Perich et al., 2018; Lowet et al., 2015)
715 and on GitHub¹⁰⁴, correspondingly.

716 References

- 717 Abramson, I. (1982). On bandwidth variation in kernel estimates—a square root law. *The annals of Statistics* ,
718 1217–1223
- 719 Aertsen, A., Bonhoeffer, T., and Krüger, J. (1987). Coherent activity in neuronal populations: analysis and
720 interpretation. *Physics of cognitive processes* , 1–34doi:10.1523/JNEUROSCI.23-17-06798.2003
- 721 Baccalá, L. and Sameshima, K. (2001). Partial directed coherence: a new concept in neural structure
722 determination. *Biological cybernetics* 84, 463–474. doi:10.1007/PL00007990
- 723 Barnett, L. and Seth, A. (2014). The MVGC multivariate Granger causality toolbox: a new approach to
724 Granger-causal inference. *Journal of neuroscience methods* 223, 50–68. doi:10.1016/j.jneumeth.2013.10.
725 018
- 726 Bastos, A. and Schoffelen, J.-M. (2016). A tutorial review of functional connectivity analysis methods and
727 their interpretational pitfalls. *Frontiers in systems neuroscience* 9, 175. doi:10.3389/fnsys.2015.00175
- 728 Benjamin, A., Fernandes, H., Tomlinson, T., Ramkumar, P., VerSteeg, C., Chowdhury, R., et al. (2018).
729 Modern machine learning as a benchmark for fitting neural responses. *Frontiers in computational*
730 *neuroscience* 12. doi:10.3389/fncom.2018.00056
- 731 Blinowska, K. (2011). Review of the methods of determination of directed connectivity from multichannel
732 data. *Medical & biological engineering & computing* 49, 521–529. doi:10.1007/s11517-011-0739-x
- 733 Bokil, H., Andrews, P., Kulkarni, J., Mehta, S., and Mitra, P. (2010). Chronux: a platform for analyzing
734 neural signals. *Journal of neuroscience methods* 192, 146–151. doi:10.1016/j.jneumeth.2010.06.020
- 735 Bonomini, M., Ferrandez, J., Bolea, J., and Fernandez, E. (2005). DATA-MEAns: an open source tool for
736 the classification and management of neural ensemble recordings. *Journal of neuroscience methods* 148,
737 137–146. doi:10.1016/j.jneumeth.2005.04.008
- 738 Brovelli, A., Ding, M., Ledberg, A., Chen, Y., Nakamura, R., and Bressler, S. (2004). Beta oscillations
739 in a large-scale sensorimotor cortical network: directional influences revealed by granger causality.
740 *Proceedings of the National Academy of Sciences* 101, 9849–9854. doi:10.1073/pnas.0308538101
- 741 Brown, E., Kass, R., and Mitra, P. (2004). Multiple neural spike train data analysis: state-of-the-art and
742 future challenges. *Nature neuroscience* 7, 456. doi:10.1038/nn1228

¹⁰⁴<https://github.com/ValentinaUn/Testing-open-source-toolboxes>

- 743 Bruns, A. (2004). Fourier-, Hilbert- and wavelet-based signal analysis: are they really different approaches?
744 *Journal of neuroscience methods* 137, 321–332
- 745 Butts, D., Weng, C., Jin, J., Alonso, J.-M., and Paninski, L. (2011). Temporal precision in the visual
746 pathway through the interplay of excitation and stimulus-driven suppression. *Journal of Neuroscience* 31,
747 11313–11327. doi:10.1523/JNEUROSCI.0434-11.2011
- 748 Cajigas, I., Malik, W., and Brown, E. (2012). nSTAT: open-source neural spike train analysis toolbox for
749 Matlab. *Journal of neuroscience methods* 211, 245–264. doi:10.1016/j.jneumeth.2012.08.009
- 750 Canolty, R., Edwards, E., Dalal, S., Soltani, M., Nagarajan, S., and Kirsch, H. e. a. (2006). High gamma
751 power is phase-locked to theta oscillations in human neocortex. *science* 313, 1626–1628. doi:10.1126/
752 science.1128115
- 753 Carter, G. (1987). Coherence and time delay estimation. *Proceedings of the IEEE* 75, 236–255. doi:
754 10.1109/PROC.1987.13723
- 755 Chakrabarti, S., Martinez-Vazquez, P., and Gail, A. (2014). Synchronization patterns suggest different
756 functional organization in parietal reach region and the dorsal premotor cortex. *American Journal of*
757 *Physiology-Heart and Circulatory Physiology* doi:10.1152/jn.00621.2013
- 758 Chicharro, D., Kreuz, T., and Andrzejak, R. (2011). What can spike train distances tell us about the neural
759 code? *Journal of neuroscience methods* 199, 146–165. doi:10.1016/j.jneumeth.2011.05.002
- 760 Cohen, M. and Kohn, A. (2011). Measuring and interpreting neuronal correlations. *Nature neuroscience* 14,
761 811. doi:10.1038/nn.2842
- 762 Cover, T. and Thomas, J. (2012). *Elements of information theory* (John Wiley & Sons). doi:10.1002/
763 047174882X
- 764 Cowley, B., Kaufman, M., Butler, Z., Churchland, M., Ryu, S., Shenoy, K., et al. (2013). DataHigh: graphical
765 user interface for visualizing and interacting with high-dimensional neural activity. *Journal of neural*
766 *engineering* 10, 066012. doi:10.1088/1741-2560/10/6/066012
- 767 Cowley, B., Semedo, J., Zandvakili, A., Smith, M., Kohn, A., and Yu, B. (2017). Distance covariance
768 analysis. In *Artificial Intelligence and Statistics*. 242–251
- 769 Cui, J., Xu, L., Bressler, S., Ding, M., and Liang, H. (2008). BSMART: a Matlab/C toolbox for analysis of
770 multichannel neural time series. *Neural Networks* 21, 1094–1104. doi:10.1016/j.neunet.2008.05.007
- 771 Cunningham, J. and Byron, M. (2014). Dimensionality reduction for large-scale neural recordings. *Nature*
772 *neuroscience* 17, 1500. doi:10.1038/nn.3776
- 773 Cutts, C. and Eglén, S. (2014). Detecting pairwise correlations in spike trains: an objective comparison
774 of methods and application to the study of retinal waves. *Journal of Neuroscience* 34, 14288–14303.
775 doi:10.1523/JNEUROSCI.2767-14.2014
- 776 Delorme, A., Mullen, T., Kothe, C., Acar, Z., Bigdely-Shamlo, N., Vankov, A., et al. (2011). EEGLAB,
777 SIFT, NFT, BCILAB, and ERICA: new tools for advanced EEG processing. *Computational intelligence*
778 *and neuroscience* 2011, 10. doi:10.1155/2011/130714
- 779 Deng, X., Eskandar, E., and Eden, U. (2013). A point process approach to identifying and tracking transitions
780 in neural spiking dynamics in the subthalamic nucleus of Parkinson’s patients. *Chaos: An Interdisciplinary*
781 *Journal of Nonlinear Science* 23, 046102. doi:10.1063/1.4818546

- 782 Egert, U., Knott, T., Schwarz, C., Nawrot, M., Brandt, A., Rotter, S., et al. (2002). MEA-Tools: an open
783 source toolbox for the analysis of multi-electrode data with MATLAB. *Journal of neuroscience methods*
784 117, 33–42. doi:10.1016/S0165-0270(02)00045-6
- 785 Farge, M. (1992). Wavelet transforms and their applications to turbulence. *Annual review of fluid mechanics*
786 24, 395–458. doi:10.1146/annurev.fl.24.010192.002143
- 787 Fee, M., Mitra, P., and Kleinfeld, D. (1996). Automatic sorting of multiple unit neuronal signals in the
788 presence of anisotropic and non-Gaussian variability. *Journal of neuroscience methods* 69, 175–188.
789 doi:10.1016/S0165-0270(96)00050-7
- 790 Fries, P., Reynolds, J., Rorie, A., and Desimone, R. (2001). Modulation of oscillatory neuronal synchroniza-
791 tion by selective visual attention. *Science* 291, 1560–1563. doi:10.1126/science.291.5508.1560
- 792 Garcia, S. and Fourcaud-Trocme, N. (2009). OpenElectrophy: an electrophysiological data-and analysis-
793 sharing framework. *Frontiers in neuroinformatics* 3, 14. doi:10.3389/neuro.11.014.2009
- 794 Garcia, S., Guarino, D., Jaillet, F., Jennings, T., Pröpper, R., Rautenberg, P., et al. (2014). Neo: an object
795 model for handling electrophysiology data in multiple formats. *Frontiers in neuroinformatics* 8, 10.
796 doi:10.3389/fninf.2014.00010
- 797 Geweke, J. (1982). Measurement of linear dependence and feedback between multiple time series. *Journal*
798 *of the American statistical association* 77, 304–313. doi:10.2307/2287238
- 799 Glaser, J., Perich, M., Ramkumar, P., Miller, L., and Kording, K. (2018). Population coding of conditional
800 probability distributions in dorsal premotor cortex. *Nature communications* 9, 1788. doi:10.1038/s41467-
801 018-04062-6
- 802 Goldberg, D., Victor, J., Gardner, E., and Gardner, D. (2009). Spike train analysis toolkit: enabling
803 wider application of information-theoretic techniques to neurophysiology. *Neuroinformatics* 7, 165–178.
804 doi:10.1007/s12021-009-9049-y
- 805 Granger, C. (1969). Investigating causal relations by econometric models and cross-spectral methods.
806 *Econometrica: Journal of the Econometric Society* , 424–438doi:10.2307/1912791
- 807 Granlund, J. (1949). Interference in frequency-modulation reception
- 808 Grün, S., Diesmann, M., and Aertsen, A. (2002). Unitary events in multiple single-neuron spiking activity: I.
809 detection and significance. *Neural Computation* 14, 43–80. doi:10.1162/089976602753284455
- 810 Grün, S., Diesmann, M., Grammont, F., Riehle, A., and Aertsen, A. (1999). Detecting unitary events without
811 discretization of time. *Journal of neuroscience methods* 94, 67–79. doi:10.1016/S0165-0270(99)00126-0
- 812 Hafner, C. and Herwartz, H. (2008). Testing for causality in variance using multivariate GARCH models.
813 *Annales d’Economie et de Statistique* , 215–241doi:10.2307/27715168
- 814 Hayden, B., Smith, D., and Platt, M. (2009). Electrophysiological correlates of default-mode processing in
815 macaque posterior cingulate cortex. *Proceedings of the National Academy of Sciences* 106, 5948–5953.
816 doi:10.1073/pnas.0812035106
- 817 Hazan, L., Zugaro, M., and Buzsáki, G. (2006). Klusters, NeuroScope, NDManager: a free software suite
818 for neurophysiological data processing and visualization. *Journal of neuroscience methods* 155, 207–216.
819 doi:10.1016/j.jneumeth.2006.01.017
- 820 Hill, D., Mehta, S., and Kleinfeld, D. (2011). Quality metrics to accompany spike sorting of extracellular
821 signals. *Journal of Neuroscience* 31, 8699–8705. doi:10.1523/JNEUROSCI.0971-11.2011

- 822 Holt, G., Softky, W., Koch, C., and Douglas, R. (1996). Comparison of discharge variability in vitro and in
823 vivo in cat visual cortex neurons. *Journal of neurophysiology* 75, 1806–1814. doi:10.1152/jn.1996.75.5.
824 1806
- 825 Hurtado, J., Rubchinsky, L., and Sigvardt, K. (2004). Statistical method for detection of phase-locking
826 episodes in neural oscillations. *Journal of neurophysiology* 91, 1883–1898. doi:10.1152/jn.00853.2003
- 827 Hurtado, J., Rubchinsky, L., Sigvardt, K., Wheelock, V., and Pappas, C. T. (2005). Temporal evolution of
828 oscillations and synchrony in GPi/muscle pairs in Parkinson’s disease. *Journal of neurophysiology* 93,
829 1569–1584. doi:10.1152/jn.00829.2004
- 830 Ince, R. (2012). Open-source software for studying neural codes. *arXiv preprint arXiv:1207.5933* doi:
831 10.1201/b14756-35
- 832 Ince, R., Mazzoni, A., Petersen, R., and Panzeri, S. (2010). Open source tools for the information theoretic
833 analysis of neural data. *Frontiers in neuroscience* 3, 11. doi:10.3389/neuro.01.011.2010
- 834 Ince, R., Petersen, R., Swan, D., and Panzeri, S. (2009). Python for information theoretic analysis of neural
835 data. *Frontiers in Neuroinformatics* 3, 4. doi:10.3389/neuro.11.004.2009
- 836 Jarvis, M. and Mitra, P. (2001). Sampling properties of the spectrum and coherency of sequences of action
837 potentials. *Neural Computation* 13, 717–749. doi:10.1162/089976601300014312
- 838 Kaminski, M. and Blinowska, K. (1991). A new method of the description of the information flow in the
839 brain structures. *Biological cybernetics* 65, 203–210. doi:10.1007/BF00198091
- 840 Kobak, D., Brendel, W., Constantinidis, C., Feierstein, C., Kepecs, A., Mainen, Z., et al. (2016). Demixed
841 principal component analysis of neural population data. *Elife* 5, e10989. doi:10.7554/eLife.10989
- 842 Kramer, M. and Eden, U. (2016). *Case Studies in Neural Data Analysis: A Guide for the Practicing*
843 *Neuroscientist* (MIT Press)
- 844 Kreuz, T., Chicharro, D., Houghton, C., Andrzejak, R., and Mormann, F. (2012). Monitoring spike train
845 synchrony. *Journal of neurophysiology* 109, 1457–1472. doi:10.1152/jn.00873.2012
- 846 Kreuz, T., Haas, J., Morelli, A., Abarbanel, H., and Politi, A. (2007). Measuring spike train synchrony.
847 *Journal of neuroscience methods* 165, 151–161. doi:10.1016/j.jneumeth.2007.05.031
- 848 Kreuz, T., Mulansky, M., and Bozanic, N. (2015). SPIKY: A graphical user interface for monitoring spike
849 train synchrony. *Journal of neurophysiology* 113, 3432–3445. doi:10.1152/jn.00848.2014
- 850 Lachaux, J.-P., Rodriguez, E., Martinerie, J., and Varela, F. (1999). Measuring phase synchrony in brain
851 signals. *Human brain mapping* 8, 194–208. doi:10.1002/(SICI)1097-0193(1999)8:4<194::AID-HBM4>3.
852 0.CO;2-C
- 853 Lakshmanan, K., Sadtler, P., Tyler-Kabara, E., Batista, A., and Yu, B. (2015). Extracting low-dimensional
854 latent structure from time series in the presence of delays. *Neural computation* 27, 1825–1856. doi:
855 10.1162/NECO.a.00759
- 856 Lawlor, P., Perich, M., Miller, L., and Kording, K. (2018). Linear-nonlinear-time-warp-poisson models of
857 neural activity. *Journal of computational neuroscience* 45, 173–191. doi:10.1007/s10827-018-0696-6
- 858 Le Van Quyen, M., Foucher, J., Lachaux, J.-P., Rodriguez, E., Lutz, A., Martinerie, J., et al. (2001).
859 Comparison of Hilbert transform and wavelet methods for the analysis of neuronal synchrony. *Journal of*
860 *neuroscience methods* 111, 83–98. doi:10.1016/S0165-0270(01)00372-7

- 861 Lidierth, M. (2009). sigTOOL: a MATLAB-based environment for sharing laboratory-developed software to
862 analyze biological signals. *Journal of neuroscience methods* 178, 188–196. doi:10.1016/j.jneumeth.2008.
863 11.004
- 864 Lindner, M., Vicente, R., Priesemann, V., and Wibral, M. (2011). TRENTOOL: A Matlab open source
865 toolbox to analyse information flow in time series data with transfer entropy. *BMC neuroscience* 12, 119.
866 doi:10.1186/1471-2202-12-119
- 867 Liu, X.-Q., Wu, X., and Liu, C. (2011). SPKtool: An open source toolbox for electrophysiological data
868 processing. In *Biomedical Engineering and Informatics (BMEI), 2011 4th International Conference on*
869 (IEEE), vol. 2, 854–857. doi:10.1109/BMEI.2011.6098451
- 870 Lizier, J. (2014). JIDT: An information-theoretic toolkit for studying the dynamics of complex systems.
871 *Frontiers in Robotics and AI* 1, 11. doi:10.3389/frobt.2014.00011
- 872 Loader, C. (2006). *Local regression and likelihood* (Springer Science & Business Media). doi:10.1007/
873 b98858
- 874 [Dataset] Lowet, E., Roberts, M., Hadjipapas, A., Peter, A., van der Eerden, J., and De Weerd, P. (2015). Data
875 from: Input-dependent frequency modulation of cortical gamma oscillations shapes spatial synchronization
876 and enables phase coding. <https://datadryad.org/resource/doi:10.5061/dryad.p631f>. doi:
877 <https://doi.org/10.5061/dryad.p631f>
- 878 Mackevicius, E., Bahle, A., Williams, A., Gu, S., Denisenko, N., Goldman, M., et al. (2019). Unsupervised
879 discovery of temporal sequences in high-dimensional datasets, with applications to neuroscience. *eLife* 8,
880 e38471. doi:10.7554/eLife.38471
- 881 Magri, C., Whittingstall, K., Singh, V., Logothetis, N., and Panzeri, S. (2009). A toolbox for the fast
882 information analysis of multiple-site LFP, EEG and spike train recordings. *BMC neuroscience* 10, 81.
883 doi:10.1186/1471-2202-10-81
- 884 Mahmud, M., Bertoldo, A., Girardi, S., Maschietto, M., and Vassanelli, S. (2012). SigMate: a Matlab-based
885 automated tool for extracellular neuronal signal processing and analysis. *Journal of neuroscience methods*
886 207, 97–112. doi:10.1016/j.jneumeth.2012.03.009
- 887 Mahmud, M. and Vassanelli, S. (2016). Processing and analysis of multichannel extracellular neuronal
888 signals: State-of-the-art and challenges. *Frontiers in neuroscience* 10, 248. doi:10.3389/fnins.2016.00248
- 889 Makino, H., Ren, C., Liu, H., Kim, A., Kondapaneni, N., Liu, X., et al. (2017). Transformation of cortex-wide
890 emergent properties during motor learning. *Neuron* 94, 880–890. doi:10.1016/j.neuron.2017.04.015
- 891 Maris, E., Schoffelen, J.-M., and Fries, P. (2007). Nonparametric statistical testing of coherence differences.
892 *Journal of neuroscience methods* 163, 161–175. doi:10.1016/j.jneumeth.2007.02.011
- 893 McFarland, J., Cui, Y., and Butts, D. (2013). Inferring nonlinear neuronal computation based on physiologi-
894 cally plausible inputs. *PLoS computational biology* 9, e1003143. doi:10.1371/journal.pcbi.1003143
- 895 Meier, R., Egert, U., Aertsen, A., and Nawrot, M. (2008). FIND – a unified framework for neural data
896 analysis. *Neural Networks* 21, 1085–1093. doi:10.1016/j.neunet.2008.06.019
- 897 Mewett, D., Reynolds, K., and Nazeran, H. (2004). Reducing power line interference in digitised elec-
898 tromyogram recordings by spectrum interpolation. *Medical and Biological Engineering and Computing*
899 42, 524–531. doi:10.1007/BF02350994
- 900 Mitra, P. (2007). *Observed brain dynamics* (Oxford University Press)

- 901 Mitra, P. and Pesaran, B. (1999). Analysis of dynamic brain imaging data. *Biophysical journal* 76, 691–708.
902 doi:10.1016/S0006-3495(99)77236-X
- 903 Montalto, A., Faes, L., and Marinazzo, D. (2014). MuTE: a MATLAB toolbox to compare established and
904 novel estimators of the multivariate transfer entropy. *PLoS one* 9, e109462. doi:10.1371/journal.pone.
905 0109462
- 906 Moore, D., Valentini, G., Walker, S., and Levin, M. (2017). Inform: A toolkit for information-theoretic
907 analysis of complex systems. In *Computational Intelligence (SSCI), 2017 IEEE Symposium Series on*
908 *(IEEE)*, 1–8. doi:10.1109/SSCI.2017.8285197
- 909 Morel, P. (2018). Gramm: grammar of graphics plotting for Matlab. *The Journal of Open Source Software* 3.
910 doi:10.21105/joss.00568
- 911 Mulansky, M., Bozanic, N., Sburlea, A., and Kreuz, T. (2015). A guide to time-resolved and parameter-free
912 measures of spike train synchrony. In *Event-based Control, Communication, and Signal Processing*
913 *(EBCCSP), 2015 International Conference on (IEEE)*, 1–8. doi:10.1186/1471-2202-16-S1-P133
- 914 Mullen, T. (2014). *The dynamic brain: Modeling neural dynamics and interactions from human electrophys-*
915 *iological recordings* (University of California, San Diego)
- 916 Niso, G., Bruña, R., Pereda, E., Gutiérrez, R., Bajo, R., Maestú, F., et al. (2013). Hermes: towards
917 an integrated toolbox to characterize functional and effective brain connectivity. *Neuroinformatics* 11,
918 405–434. doi:10.1007/s12021-013-9186-1
- 919 Nolte, G., Bai, O., Wheaton, L., Mari, Z., Vorbach, S., and Hallett, M. (2004). Identifying true brain
920 interaction from EEG data using the imaginary part of coherency. *Clinical neurophysiology* 115, 2292–
921 2307. doi:10.1016/j.clinph.2004.04.029
- 922 Nolte, G., Ziehe, A., Nikulin, V., Schlögl, A., Krämer, N., Brismar, T., et al. (2008). Robustly estimating
923 the flow direction of information in complex physical systems. *Physical review letters* 100, 234101.
924 doi:10.1103/PhysRevLett.100.234101
- 925 Oostenveld, R., Fries, P., Maris, E., and Schoffelen, J.-M. (2011). FieldTrip: open source software for
926 advanced analysis of MEG, EEG, and invasive electrophysiological data. *Computational intelligence and*
927 *neuroscience* 2011, 1. doi:10.1155/2011/156869
- 928 Özkurt, T. and Schnitzler, A. (2011). A critical note on the definition of phase–amplitude cross-frequency
929 coupling. *Journal of Neuroscience methods* 201, 438–443. doi:10.1016/j.jneumeth.2011.08.014
- 930 Pachitariu, M., Steinmetz, N., Kadir, S., Carandini, M., and Harris, K. (2016). Fast and accurate spike sorting
931 of high-channel count probes with KiloSort. In *Advances in Neural Information Processing Systems*.
932 4448–4456
- 933 Paninski, L., Pillow, J., and Lewi, J. (2007). Statistical models for neural encoding, decoding, and optimal
934 stimulus design. *Progress in brain research* 165, 493–507. doi:10.1016/S0079-6123(06)65031-0
- 935 Parikh, H. (2009). *On Improving the Effectiveness of Control Signals from Chronic Microelectrodes for*
936 *Cortical Neuroprostheses*. Ph.D. thesis
- 937 Park, I., Meister, M., Huk, A., and Pillow, J. (2014). Encoding and decoding in parietal cortex during
938 sensorimotor decision-making. *Nature neuroscience* 17, 1395. doi:10.1038/nn.3800
- 939 Park, I. and Pillow, J. (2011). Bayesian spike-triggered covariance analysis. In *Advances in neural information*
940 *processing systems*. 1692–1700

- 941 Pastore, V., Poli, D., Godjoski, A., Martinoia, S., and Massobrio, P. (2016). ToolConnect: a functional
942 connectivity toolbox for in vitro networks. *Frontiers in neuroinformatics* 10, 13. doi:10.3389/fninf.2016.
943 00013
- 944 Percival, D. and Walden, A. (1993). *Spectral analysis for physical applications* (Cambridge University
945 Press). doi:10.1017/CBO9780511622762
- 946 [Dataset] Perich, M., Lawlor, P., Miller, L., and Kording, K. (2018). Extracellular neural recordings
947 from macaque primary and dorsal premotor motor cortex during a sequential reaching task. [http://](http://crcns.org/data-sets/motor-cortex/pmd-1)
948 crcns.org/data-sets/motor-cortex/pmd-1. doi:10.6080/K0FT8J72
- 949 Pesaran, B. (2008). Spectral analysis for neural signals. In *Short course III, presented at 2008 Society for*
950 *Neuroscience Annual Meeting (Mitra P.P., ed.)*
- 951 Pettersen, K., Devor, A., Ulbert, I., Dale, A., and Einevoll, G. (2006). Current-source density estimation based
952 on inversion of electrostatic forward solution: effects of finite extent of neuronal activity and conductivity
953 discontinuities. *Journal of neuroscience methods* 154, 116–133. doi:10.1016/j.jneumeth.2005.12.005
- 954 Pillow, J., Shlens, J., Paninski, L., Sher, A., Litke, A., Chichilnisky, E., et al. (2008). Spatio-temporal
955 correlations and visual signalling in a complete neuronal population. *Nature* 454, 995. doi:10.1038/
956 nature07140
- 957 Pouzat, C. and Chaffiol, A. (2009). Automatic spike train analysis and report generation. an implementation
958 with r, r2html and star. *Journal of neuroscience methods* 181, 119–144. doi:10.1016/j.jneumeth.2009.01.
959 037
- 960 Prechtl, J., Cohen, L., Pesaran, B., Mitra, P., and Kleinfeld, D. (1997). Visual stimuli induce waves of
961 electrical activity in turtle cortex. *Proceedings of the National Academy of Sciences* 94, 7621–7626
- 962 Prieto, G., Parker, R., Thomson, D., Vernon, F., and Graham, R. (2007). Reducing the bias of multitaper
963 spectrum estimates. *Geophysical Journal International* 171, 1269–1281
- 964 Pröpper, R. and Obermayer, K. (2013). Spyke Viewer: a flexible and extensible platform for electrophysio-
965 logical data analysis. *Frontiers in neuroinformatics* 7, 26. doi:10.3389/fninf.2013.00026
- 966 Quaglio, P., Rostami, V., Torre, E., and Grün, S. (2018). Methods for identification of spike patterns in
967 massively parallel spike trains. *Biological cybernetics* 112, 57–80. doi:10.1007/s00422-018-0755-0
- 968 Quaglio, P., Yegenoglu, A., Torre, E., Endres, D., and Grün, S. (2017). Detection and evaluation of spatio-
969 temporal spike patterns in massively parallel spike train data with SPADE. *Frontiers in computational*
970 *neuroscience* 11, 41. doi:10.3389/fncom.2017.00041
- 971 Quiroga, R., Kreuz, T., and Grassberger, P. (2002). Event synchronization: a simple and fast method to
972 measure synchronicity and time delay patterns. *Physical review E* 66, 041904. doi:10.1103/PhysRevE.66.
973 041904
- 974 Quiroga, R., Nadasdy, Z., and Ben-Shaul, Y. (2004). Unsupervised spike detection and sorting with
975 wavelets and superparamagnetic clustering. *Neural computation* 16, 1661–1687. doi:10.1162/
976 089976604774201631
- 977 Rankine, L., Stevenson, N., Mesbah, M., and Boashash, B. (2005). A quantitative comparison of non-
978 parametric time-frequency representations. In *2005 13th European Signal Processing Conference (IEEE)*,
979 1–4

- 980 Rivlin-Etzion, M., Ritov, Y., Heimer, G., Bergman, H., and Bar-Gad, I. (2006). Local shuffling of spike
981 trains boosts the accuracy of spike train spectral analysis. *Journal of neurophysiology* 95, 3245–3256.
982 doi:10.1152/jn.00055.2005
- 983 Rosenberg, J., Amjad, A., Breeze, P., Brillinger, D., and Halliday, D. (1989). The Fourier approach to the
984 identification of functional coupling between neuronal spike trains. *Progress in biophysics and molecular*
985 *biology* 53, 1–31. doi:10.1016/0079-6107(89)90004-7
- 986 Rosenberg, J., Halliday, D., Breeze, P., and Conway, B. (1998). Identification of patterns of neuronal
987 connectivity: partial spectra, partial coherence, and neuronal interactions. *Journal of neuroscience methods*
988 83, 57–72. doi:10.1016/S0165-0270(98)00061-2
- 989 Russo, E. and Durstewitz, D. (2017). Cell assemblies at multiple time scales with arbitrary lag constellations.
990 *Elife* 6, e19428. doi:10.7554/eLife.19428
- 991 Samiee, S. and Baillet, S. (2017). Time-resolved phase-amplitude coupling in neural oscillations. *NeuroImage*
992 159, 270–279. doi:10.1016/j.neuroimage.2017.07.051
- 993 Schrader, S., Grun, S., Diesmann, M., and Gerstein, G. (2008). Detecting synfire chain activity using
994 massively parallel spike train recording. *Journal of neurophysiology* 100, 2165–2176. doi:10.1152/jn.
995 01245.2007
- 996 Scott, D. (1979). On optimal and data-based histograms. *Biometrika* 66, 605–610. doi:10.1093/biomet/66.3.
997 605
- 998 Shimazaki, H. and Shinomoto, S. (2010). Kernel bandwidth optimization in spike rate estimation. *Journal of*
999 *computational neuroscience* 29, 171–182. doi:10.1007/s10827-009-0180-4
- 1000 Shinomoto, S., Miura, K., and Koyama, S. (2005). A measure of local variation of inter-spike intervals.
1001 *Biosystems* 79, 67–72. doi:10.1016/j.biosystems.2004.09.023
- 1002 Shinomoto, S., Shima, K., and Tanji, J. (2003). Differences in spiking patterns among cortical neurons.
1003 *Neural Computation* 15, 2823–2842. doi:10.1162/089976603322518759
- 1004 Shlens, J. (2014). A tutorial on principal component analysis. *arXiv preprint arXiv:1404.1100*
- 1005 Slepian, D. and Pollak, H. (1961). Prolate spheroidal wave functions, Fourier analysis and uncertainty I. *Bell*
1006 *System Technical Journal* 40, 43–63. doi:10.1002/j.1538-7305.1964.tb01037.x
- 1007 Stam, C., Nolte, G., and Daffertshofer, A. (2007). Phase lag index: assessment of functional connectivity
1008 from multi channel EEG and MEG with diminished bias from common sources. *Human brain mapping*
1009 28, 1178–1193. doi:10.1002/hbm.20346
- 1010 Staude, B., Rotter, S., and Grün, S. (2010). CuBIC: cumulant based inference of higher-order correlations in
1011 massively parallel spike trains. *Journal of computational neuroscience* 29, 327–350. doi:10.1007/s10827-
1012 009-0195-x
- 1013 Stevenson, I. and Kording, K. (2011). How advances in neural recording affect data analysis. *Nature*
1014 *neuroscience* 14, 139. doi:10.1038/nn.2731
- 1015 Stoica, P., Moses, R., et al. (2005). *Spectral analysis of signals* (Pearson Prentice Hall Upper Saddle River,
1016 NJ)
- 1017 Tadel, F., Baillet, S., Mosher, J., Pantazis, D., and Leahy, R. (2011). Brainstorm: a user-friendly application
1018 for MEG/EEG analysis. *Computational intelligence and neuroscience* 2011, 8. doi:10.1155/2011/879716

- 1019 Tallon-Baudry, C., Bertrand, O., Delpuech, C., and Pernier, J. (1997). Oscillatory γ -band (30–70 Hz)
1020 activity induced by a visual search task in humans. *Journal of Neuroscience* 17, 722–734. doi:10.1523/
1021 JNEUROSCI.17-02-00722.1997
- 1022 Thomson, D. (1982). Spectrum estimation and harmonic analysis. *Proceedings of the IEEE* 70, 1055–1096.
1023 doi:10.1109/PROC.1982.12433
- 1024 Timme, N. and Lapish, C. (2018). A tutorial for information theory in neuroscience. *eNeuro* 5. doi:
1025 10.1523/ENEURO.0052-18.2018
- 1026 Torre, E., Canova, C., Denker, M., Gerstein, G., Helias, M., and Grün, S. (2016). ASSET: analysis of
1027 sequences of synchronous events in massively parallel spike trains. *PLoS computational biology* 12,
1028 e1004939. doi:10.1371/journal.pcbi.1004939
- 1029 Torre, E., Picado-Muiño, D., Denker, M., Borgelt, C., and Grün, S. (2013). Statistical evaluation of
1030 synchronous spike patterns extracted by frequent item set mining. *Frontiers in computational neuroscience*
1031 7, 132. doi:10.3389/fncom.2013.00132
- 1032 Tort, A., Komorowski, R., Eichenbaum, H., and Kopell, N. (2010). Measuring phase-amplitude coupling
1033 between neuronal oscillations of different frequencies. *Journal of neurophysiology* 104, 1195–1210.
1034 doi:10.1152/jn.00106.2010
- 1035 Truccolo, W., Eden, U., Fellows, M., Donoghue, J., and Brown, E. (2005). A point process framework for
1036 relating neural spiking activity to spiking history, neural ensemble, and extrinsic covariate effects. *Journal*
1037 *of neurophysiology* 93, 1074–1089. doi:10.1152/jn.00697.2004
- 1038 van Rossum, M. (2001). A novel spike distance. *Neural computation* 13, 751–763. doi:10.1162/
1039 089976601300014321
- 1040 van Vugt, M., Sederberg, P., and Kahana, M. (2007). Comparison of spectral analysis methods for characteriz-
1041 ing brain oscillations. *Journal of neuroscience methods* 162, 49–63. doi:10.1016/j.jneumeth.2006.12.004
- 1042 Victor, J. and Purpura, K. (1996). Nature and precision of temporal coding in visual cortex: a metric-space
1043 analysis. *Journal of neurophysiology* 76, 1310–1326. doi:10.1152/jn.1996.76.2.1310
- 1044 Vinck, M., Battaglia, F., Womelsdorf, T., and Pennartz, C. (2012). Improved measures of phase-coupling
1045 between spikes and the local field potential. *Journal of computational neuroscience* 33, 53–75. doi:
1046 10.1007/s10827-011-0374-4
- 1047 Vinck, M., Oostenveld, R., Van Wingerden, M., Battaglia, F., and Pennartz, C. (2011). An improved index
1048 of phase-synchronization for electrophysiological data in the presence of volume-conduction, noise and
1049 sample-size bias. *Neuroimage* 55, 1548–1565. doi:10.1016/j.neuroimage.2011.01.055
- 1050 Vinck, M., van Wingerden, M., Womelsdorf, T., Fries, P., and Pennartz, C. (2010). The pairwise phase
1051 consistency: a bias-free measure of rhythmic neuronal synchronization. *Neuroimage* 51, 112–122.
1052 doi:10.1016/j.neuroimage.2010.01.073
- 1053 Voytek, B., Canolty, R., Shestyuk, A., Crone, N., Parvizi, J., and Knight, R. (2010). Shifts in gamma phase-
1054 amplitude coupling frequency from theta to alpha over posterior cortex during visual tasks. *Frontiers in*
1055 *human neuroscience* 4, 191. doi:10.3389/fnhum.2010.00191
- 1056 Wagenaar, D., DeMarse, T., and Potter, S. (2005). MeaBench: A toolset for multi-electrode data acquisition
1057 and on-line analysis. In *Neural Engineering, 2005. Conference Proceedings. 2nd International IEEE*
1058 *EMBS Conference on (IEEE)*, 518–521. doi:10.1109/CNE.2005.1419673

- 1059 Williams, A., Kim, T., Wang, F., Vyas, S., Ryu, S., and Shenoy, K. e. a. (2018). Unsupervised discovery of
1060 demixed, low-dimensional neural dynamics across multiple timescales through tensor component analysis.
1061 *Neuron* doi:10.1016/j.neuron.2018.05.015
- 1062 Wong, R., Meister, M., and Shatz, C. (1993). Transient period of correlated bursting activity during
1063 development of the mammalian retina. *Neuron* 11, 923–938. doi:10.1016/0896-6273(93)90122-8
- 1064 Yegenoglu, A., Holstein, D., Phan, L., Denker, M., Davison, A., and Grün, S. (2017). Elephant–open-source
1065 tool for the analysis of electrophysiological data sets. In *Bernstein Conference 2015: Abstract Book*.
1066 W–05. doi:10.12751/nncn.bc2015.0126
- 1067 Yu, B., Cunningham, J., Santhanam, G., Ryu, S., Shenoy, K., and Sahani, M. (2009). Gaussian-process factor
1068 analysis for low-dimensional single-trial analysis of neural population activity. In *Advances in neural*
1069 *information processing systems*. 1881–1888. doi:10.1152/jn.90941.2008